# Posterior Fossa Malformations

*Nolan R. Altman,*[1] *Thomas P. Naidich, and Bruce H. Braffman*

From the Miami Children's Hospital (NAA), the Baptist Hospital of Miami (TPN), and the Memorial Hospital, Hollywood, FL (BHB)

Posterior fossa malformations are best classified in terms of their embryogenesis from the rhombencephalon (1–7). The diverse manifestations of the dysgeneses can be related to the stages at which development of the cerebellum became deranged. The cerebellar malformations can also be classified by their effect on the fourth ventricle and cisterna magna, and by whether any cystic spaces represent expansion of the rhombencephalic vesicle or secondary atrophy of the parenchyma. Since the size of the posterior fossa depends largely on the size of the rhombencephalic vesicle at the time that the mesenchyme condenses into the bony-dural walls of the posterior fossa (see article by McLone in this issue), identification of the size of the posterior fossa often proves to be more helpful in differentiating among these malformations than the simple presence, or absence, of a cyst. In this discussion, the Chiari malformations have been specifically excluded since they have been addressed previously (8–17).

## Definitions

The normal mature cerebellum is divided into three lobes: anterior, posterior, and flocculonodular (Fig. 1).

A. The anterior lobe consists of the first three lobules of vermis with their lateral extension into the hemispheres, ie,

| vermis | and | hemispheres |
|---|---|---|
| 1. lingula, | with | no hemispheric portion in man |
| 2. central lobule | with | the two alae, and |
| 3. culmen | with the | (anterior) quadrangular lobule. |

The anterior lobe is the most rostral portion of the cerebellum and is separated from the more caudal portions of the cerebellum by the primary fissure.

B. The posterior lobe consists of the next five lobules of the vermis with their hemispheric connections, ie,

| vermis | and | hemispheres |
|---|---|---|
| 4. declive | with the | lobulus simplex |
| 5. folium | with the | superior semilunar lobule |
| 6. tuber and | with the | inferior semilunar, gracile and |
| 7. pyramis | | biventral lobules |
| 8. uvula | with the | cerebellar tonsils. |

The posterior lobe is separated from the more caudal cerebellum by the posterolateral (flocculonodular) fissure. The posterior lobe undergoes the greatest growth in man receiving the influx of the pontocerebellar fibers (2).

C. The flocculonodular lobe if formed by

| vermis | and | hemispheres |
|---|---|---|
| 9. nodulus | with the | flocculi. |

Embryologically, the flocculonodular lobe forms first, when deepening of the flocculonodular fissure (synonym: posterolateral fissure) separates the flocculonodular lobe from the rest of the cerebellum that is developing rostral to it (1). The anterior lobe forms next; when deepening of the primary fissure separates the culmen of the anterior lobe from the declive of the posterior lobe (1). By approximately 4 months gestation, the main fissures and the subdivisions of the anterior and the posterior lobes of the vermis have formed (1). In general the growth of the cerebellar hemispheres lags behind the growth of the vermis by 30–60 days (1–3).

[1] Address reprint requests to Dr Altman, Department of Radiology, Miami Children's Hospital, 6125 SW 31st Street, Miami, FL 33155.

**Index terms:** Posterior fossa, abnormalities and anomalies; Pediatric neuroradiology

AJNR 13:691–724, Mar/Apr 1992 0195-6108/92/1302-0691

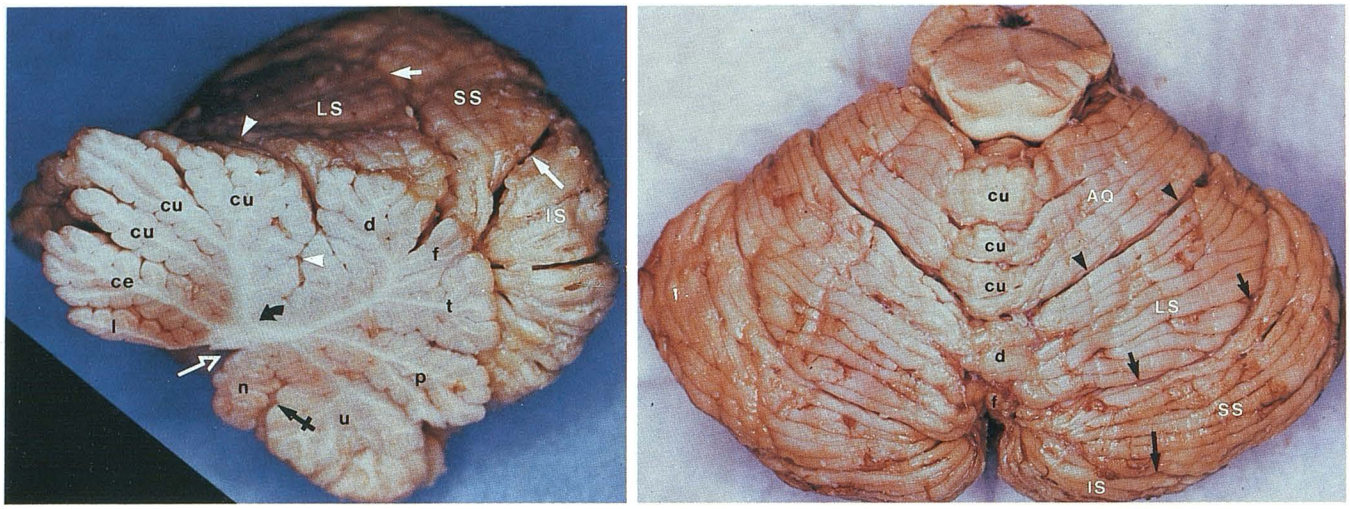


A B C D

Fig. 1. Anatomy of the mature cerebellum.

*A*, Midsagittal section of the cerebellum after removal of the brain stem.

*B–D*, Surface features of the cerebellum as seen from *B*, superior; *C*, posterior; and *D*, posteroinferior. The pia arachnoid has been removed and the fissures have been spread to emphasize their shapes and relationships. Note the fastigium (*open white arrow*) that is the superior midline point of the fourth ventricle and the white matter of the vermis (designated the arbor vitae) that appears to radiate outward from the fastigium like a starburst. The first major division (*curved black arrow*) of the arbor vitae indicates the division of the cerebellum into the anterior lobe and posterior lobe at the primary fissure (*single arrowheads*). The division to the flocculonodular lobe is not shown. The nine lobules of vermis are directly continuous laterally with the lobules of the cerebellum. The culmen is the largest lobule of vermis. The specific branching pattern of the arbor vitae helps to identify each lobule. The vermis is well defined and can be distinguished from the cerebellar hemispheres by paired paravermian grooves and by the abrupt angulation of the folia and fissures as they change from the horizontal orientation of the vermis to the oblique orientation of each hemisphere. Note the relationships of the labeled fissures to the adjacent lobules: primary fissure (*single arrowheads*), superior posterior fissure (*single short arrows*), great horizontal fissure (*single long arrows*), ansoparamedian fissure (*double arrowheads*), prebiventral fissure (*double short arrows*), intrabiventral fissure (*double long arrows*), and secondary fissure (*triple arrowheads*). The posterolateral fissure (*crossed arrow*) that separates the posterior from the flocculonodular lobes is shown only at the vermis. Vermis: *l* = lingula, *ce* = central, *cu* = culmen, *d* = declive, *f* = folium, *t* = tuber, *p* = pyramis, *u* = uvula, *n* = nodulus. Hemispheres: *AQ* = (anterior) quadrigeminal lobule, *LS* = lobulus simplex, *SS* = superior semilunar lobule, *IS* = inferior semilunar lobule, *G* = gracile lobule, *B* = biventral lobule, *T* = tonsils. The flocculi are not shown.

In recognition of this temporal sequence of development and in accord with the sequential evaluation of these structures in phylogeny, the portions of the cerebellum may also be designated the archicerebellum, paleocerebellum, and neocerebellum.

### *Archicerebellum*

The term archicerebellum designates the flocculonodular lobe (2, 3). It is the first portion of the cerebellum to differentiate and is believed to be the most primitive. Because it is concerned with the *vestibular nuclei*, it is also designated the *vestibular* cerebellum.

### *Paleocerebellum*

The term paleocerebellum designates the flocculi of the hemispheres plus the entire vermis (2). This appears to be a useful distinction, because the vermis of the anterior and posterior lobes forms before the corresponding hemispheres, so the flocculonodular lobe and the vermis coexist before the anterior and posterior lobes of the cerebellar hemispheres are well formed.

### *Neocerebellum*

The term neocerebellum designates the cerebellar hemispheres except for the flocculi (2, 3).

The cerebellar dysplasias can be classified in these terms as archicerebellar, paleocerebellar, and neocerebellar dysplasias. Paleocerebellar dysplasias have vermian defects as key features. These tend to include subtle malformations of the medulla, especially the inferior olives and the pyramidal tracts (2). Neocerebellar dysplasias involve the cerebellar hemispheres with relative sparing of the vermis and flocculi.

## Normal embryogenesis of the cerebellum

There is general agreement among the authorities as the broad order and the sequence of timing of the crucial events in embryogenesis (1–7, 18). The authorities differ substantially in the precise times at which they state specific events occur (1, 2, 18). Therefore, although every effort has been made to be accurate, the following discussion is intended more to provide an overview of cerebellar embryogenesis than to give exact dates for each single event.

The cerebellum arises by a series of steps best understood in terms of the Carnegie Stages of Development (1).

### *Stage 10*

At approximately 22 days, before the neural tube closes, two constrictions in the cephalic portion of the neural tube divide it into the prosencephalon, mesencephalon, and rhombencephalon (Fig. 2). These constrictions become more evident during stages 11 and 12 (approximately 24–27 days). The rostral neuropore closes during stage 11 (19). When the brain becomes a closed tube, the three divisions of the neural tube are designated the *primary brain vesicles.* The prosencephalon and rhombencephalon each promptly divides into two secondary vesicles. The subdivisions of the rhombencephalon are designated the metencephalon (future pons and cerebellum) and the myelencephalon (future medulla oblongata). A constricted region, the isthmus, unites the mesencephalon with the metencephalon (5).

### *Stages 13–16*

From approximately 28–37 days, the rhombencephalon flexes increasingly, convex ventrally, to form the pontine flexure (Fig. 3). As a consequence:

1. The thin roof of the rhombencephalon be-

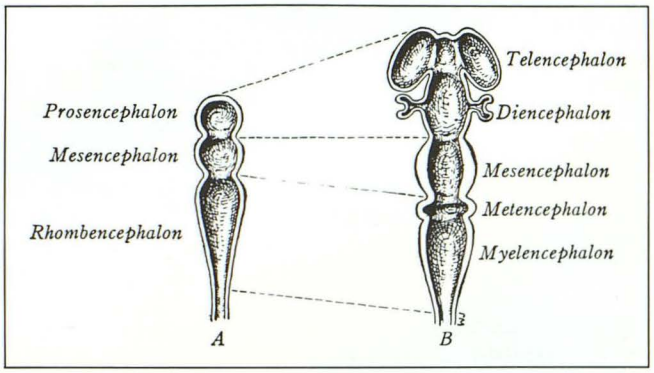


Fig. 2. Embryology; diagrammatic representation of the primary and secondary brain vesicles.

*A*, Initially the neural tube constricts to form the three primary brain vesicles. These define the hindbrain (*rhombencephalon*), the midbrain (*mesencephalon*), and the forebrain (*prosencephalon*).

*B*, Subsequently, the metencephalon and myelencephalon develop from the rhombencephalon, the telencephalon and the diencephalon develop from the prosencephalon, and the optic vesicles extend outward from the diencephalon. (Reprinted with permission from Arey (5), p. 431, Fig. 404.)

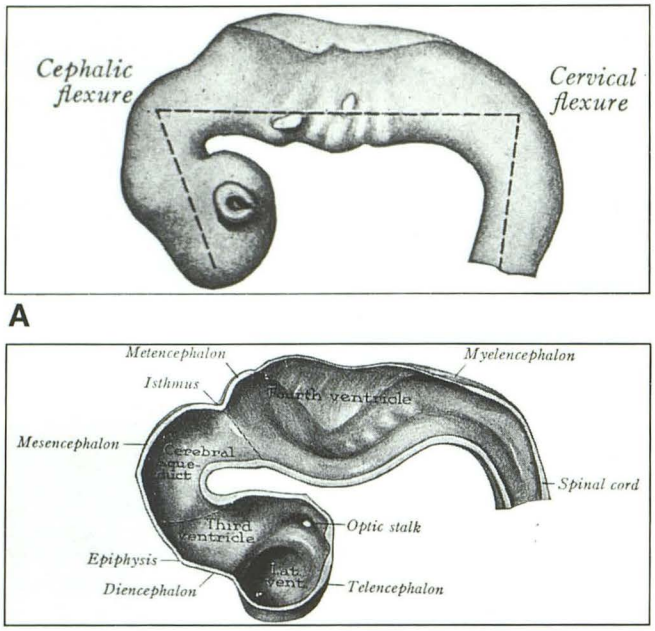


Fig. 3. Embryology; diagrammatic representation of the flexing neural tube. *A*, 6-mm stage; *B*, 11-mm stage (hemisection); *C*, 14-mm stage. (Reprinted with permission from Arey (5), p. 431, Figs. 406 and 407.)

comes folded and forms a transverse crease (the plica choroidea) that runs perpendicular to the long axis of the neural tube. The transverse crease is approximately in line with the future plane of the foramina of Luschka (Figs. 4 and 5). The choroid plexus of the fourth ventricle will develop within the transverse crease by apposition of mesoderm to ependyma (1).

2. As the pons flexes, the alar plates that form the sides of the neural tube flare laterally, so the lumen of the rhombencephalon at the level of the crease becomes the widest portion of the neural tube (Fig. 4) (1). Because of the flaring, the side walls of the rhombencephalon assume a diamond shape (as seen from posterior). From their widest separation at the transverse crease, the lips angle obliquely back toward the midline both cephalically (toward the mesencephalon) and caudally (toward the myelencephalon). A series of transient, transversely oriented rhombic grooves becomes evident along the floor of the rhombencephalic cavity from stages 10–15 (approximately 22–34 days) (Fig. 4A). These identify the intervening rhombomeres (synonym: neuromeres) that are related to the anlagen for cranial nerves 5–10. The rostral-most groove lies at the level of the pontine flexure and is related to the trigeminal nerve. The other grooves lie caudal to the pontine flexure. The first rhombencephalic segment caudal to the isthmus may be designated rhombomere 1.

*Stages 13–18*

From approximately 28–44 days, the cerebellum will arise from the alar plate of the rhombencephalon rostral to the plica choroidea (Figs. 4B, 4C, and 5) (1). That portion of the alar plate rostral to the developing trigeminal sensory nerve will form the major portion of the cerebellum. Intense neuroblastic activity causes the lateral aspects of the alar plates to hypertrophy into thick rhombic lips (1). Although the first indication of the developing cerebellar hemispheres can be seen histologically at stages 13 or 14 (6), gross morphologic development of the cerebellar hemispheres is not appreciated until stage 18 (7). At this stage, the *external* cerebellar bulge first appears along the caudal margin of the cerebellum as a transversely oriented strip of tissue that is separated from the rest of the cerebellum by a transverse groove (Figs. 4 and 5) (7). The transverse groove will become the posterolateral (flocculonodular) groove and the transverse strip will form the flocculonodular lobe. Also at this stage the *internal* cerebellar bulge first appears as a protrusion into the developing fourth ventricle. The internal bulge is derived from the alar plates of both rhombomere 1 and the isthmic segment (7). It will form the anterior and posterior lobes of the cerebellum.

According to England, the superior meduallary velum, the superior cerebellar peduncles, and the cranial part of the fourth ventricle form from the isthmus (4).

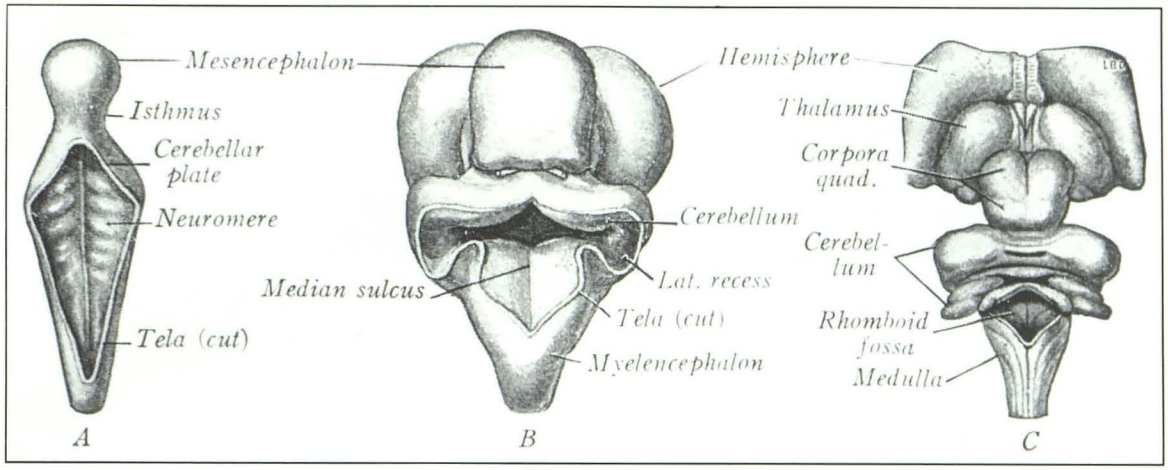


Fig. 4. Embryology; diagrammatic representation of future development of the hindbrain, as seen from behind.

*A*, 5 weeks. The neuromeres are visible along the floor of the diamond-shaped rhombencephalic vesicle. The alar plates angle medially from the widest point of the diamond toward the isthmus and toward the myelencephalon.

*B*, 9 weeks. Note the alignment of the lateral recesses and the midpoint of the fourth ventricle in a transverse plane that corresponds to the plica choroidalis. The cerebellum develops predominantly from the alar plates rostral to the plica choroidalis.

*C*, 15 weeks. Note the differentiation of the lobules of the vermis and hemispheres.

Reprinted with permission from Arey (5), p. 435, Fig. 409.)

*Stages 18–19*

During stages 18 and 19 (approximately 44 days and 48 days) the flocculi, superior cerebellar peduncles, dentate, and olivary nuclei form. The first choroid plexus becomes recognizable within the fourth ventricle (19).

The primary fissure forms at about 73 days. The individual vermian lobules can be identified by approximately 4 months gestation (Figs. 5C and 6) (1). The entire vermis is formed by the end of the 15th week (18). The hemispheres tend to lag 30–60 days behind the vermis. Eventually, hemispheric growth obscures the vermis (1). More rapid proliferation of the midregions of the cerebellum creates the typical mushroom shape (1). Marked proliferation of the cerebellar cortex and relative inactivity of the roof of the fourth ventricle causes the fastigium to assume the shape of an inverted "V" when viewed sagittally. The nodulus thus becomes tucked in and comes to lie adjacent to the apex of the fastigium (1). At birth, the human cerebellum is morphologically identical to the adult except for size. However, cellular differentiation and migration continue. (See "Embryogenis of the Cerebellar Cortex" on page 719 in this article).

The medullary vela and the choroid plexus are believed to form as follows (20): The cavity of the rhombencephalon—the rhombencephalic vesicle—expands greatly, especially anteriorly just behind the mesencephalon, to become the fourth ventricle. In the normal brain, the pontine flexure creates the transversely oriented plica choroidea that runs across the roof of the rhombencephalic vesicle (Figs. 3 and 7). This divides the roof into two membranous areas: 1) the area membranacea superior that is situated between the caudal edge of the cerebellar anlage and the plica choroidea, and 2) the area membranacea inferior that lies caudal to the plica choroidea. The area membranacea superior normally disappears by becoming incorporated into the developing choroid plexus. As a result, the choroid plexus comes to lie in direct relation to the caudal edge of the cerebellum. The area membranacea inferior will later become permeable at the foramen to Magendie.

As overgrowth of the midportion of cerebellum occurs creating the "mushroom shape" of the cerebellum: 1) the lateral edges of the choroid remain at the lateral recesses of the fourth ventricle at the site of the pontine flexure and the originally widest part of the rhombencephalic vesicle, and 2) the medial portions of the choroid plexi are displaced caudally and then rostrally by the "tucking in" of the nodulus. Thus, the choroid plexus that originally developed caudal to the cerebellum comes to lie rostral to the lower cerebellum in the final form (1, 20). In the full term

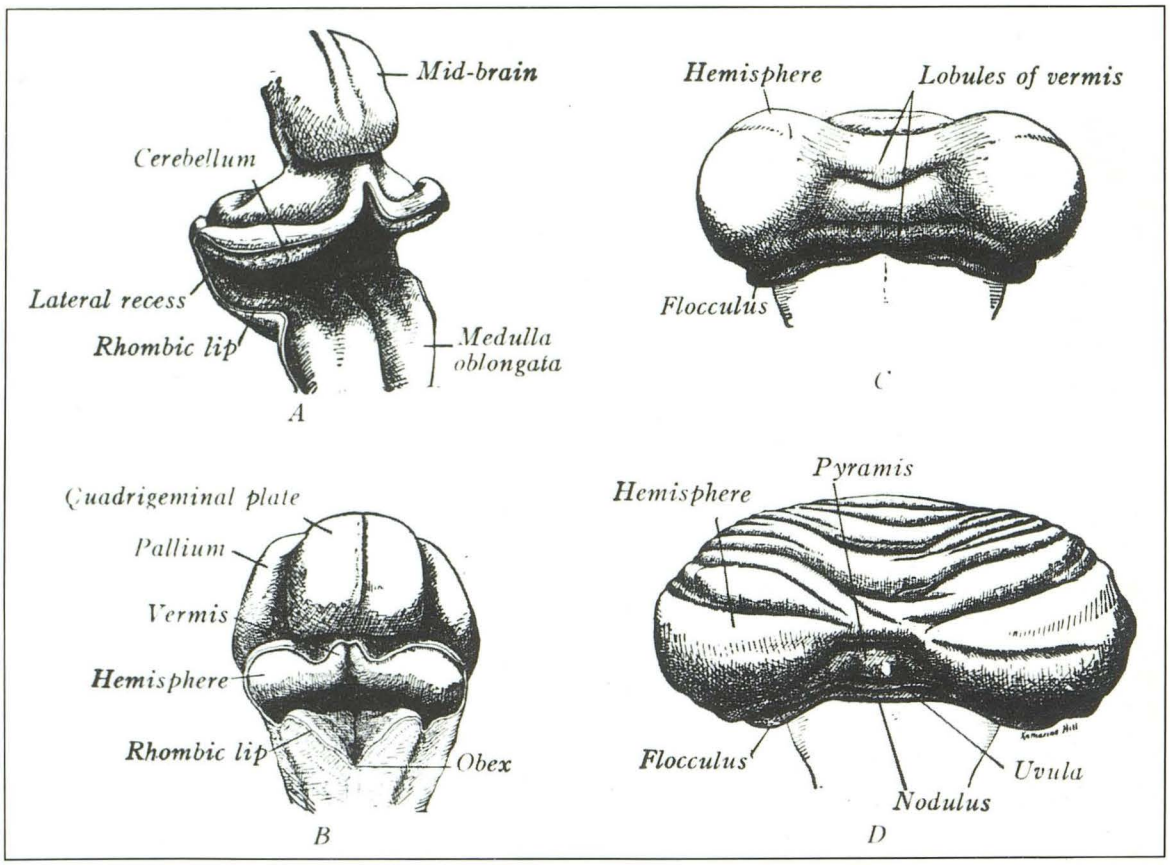


Fig. 5. Embryology; diagrammatic representation of cerebellar development.

*A*, 6 weeks; note the orientation of the lateral recesses to the pontine flexure.

*B*, 2 months; note the early formation of vermis and hemisphere.

*C*, 4 months and *D*, 5 months; note the progressive differentiation of the lobules of the cerebellum with caudal position of the flocculonodular lobe and progressive displacement of that lobe by the "mushroom" growth of the anterior and posterior lobes cephalic to it.

Reprinted with permission from Arey (5), p 441, Fig. 415.)

infant, the choroid plexus can be seen to course from the lateral recesses of the fourth ventricle (the derivation of the widest portion of the rhombic roof at the pontine flexure) toward the midline at the fastigium and then swing caudally to run into cisterna magna via the foramen of Magendie on the remnant of the posterior medullary velum (1). The foramina of Luschka appears late in the fourth month of gestation (195 mm crown-rump length) (1, 20). The time of opening of the foramen of Magendie is not established (1, 20).

## Cerebellar Pathology

### *Complete Cerebellar Aplasia*

Total cerebellar aplasia is exceedingly uncommon. Stewart (21) summarized two cases from the literature. In the first, the cerebral hemispheres were normal or slightly large. The tentorium was intact. In the space normally occupied by cerebellum, there was a gelatinous membrane connected to the medulla by two membranous pedicles. Two detached pea-like masses of white matter were observed in the neighborhood of the pedicles. The quadrigeminal plate was intact. The aqueduct was seen within softened tissue. This softening encroached on the inferior cerebellar peduncles and the olives. No fourth ventricle and no pons could be found. The medullary pyramids diverged directly into the crura cerebri.

In the second case, there was no vestige of cerebellum, peduncles, or pons. The fourth ventricle was covered by a thin (0.5 mm) sheet of tissue running from the quadrigeminal plate to the dorsal surface of the medulla. Ventrally, the

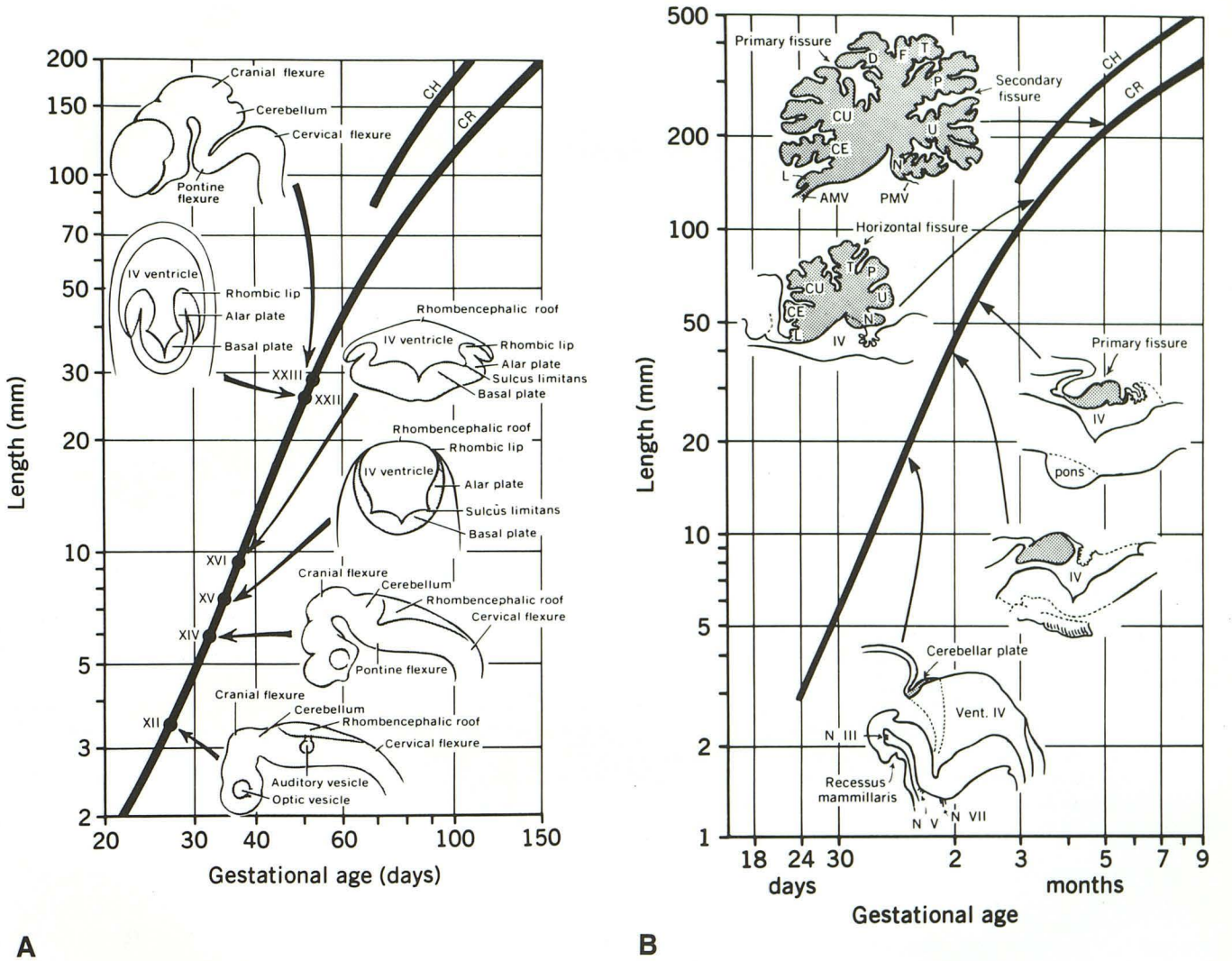


Fig. 6. *A*, and *B*, Sequential development of the cerebellum. Please note the progressive evolution of the size and configuration of the cerebellum. The precise time of each stage cannot be stated exactly and is presently under continuing reevaluation. (Reprinted with permission from Lemire et al (1).)

medullary pyramids ran up to the quadrigeminal plate. A posterior fossa was present, but there was no tentorium. The cerebrum was markedly thinned by distension of the ventricles.

In this condition, the posterior columns of the spinal cord may be separated throughout their length by an ependyma-lined cleft. The uncrossed pyramidal tracts may extend inferiorly as prominent bundles in the anterior columns of the cord (22).

Embryologically, these cases appear to result from destruction of the cerebellum. The presence of a posterior fossa in case two suggests the prior development of a hindbrain that is no longer present.

### *Paleocerebellar Dysgenesis*

The majority of cerebellar dysgeneses are paleocerebellar dysgeneses. In these, the dysgenesis of the vermis may be partial or complete. The major entities in this group are Dandy-Walker complex, Joubert syndrome, tectocerebellar dysraphia, and rhombencephalosynapsis.

### Dandy-Walker Complex

The conditions called Dandy-Walker malformation, Dandy-Walker variant, and mega cisterna magna are believed to represent a continuum of developmental anomalies designated the Dandy-Walker complex by Barkovich et al (18).

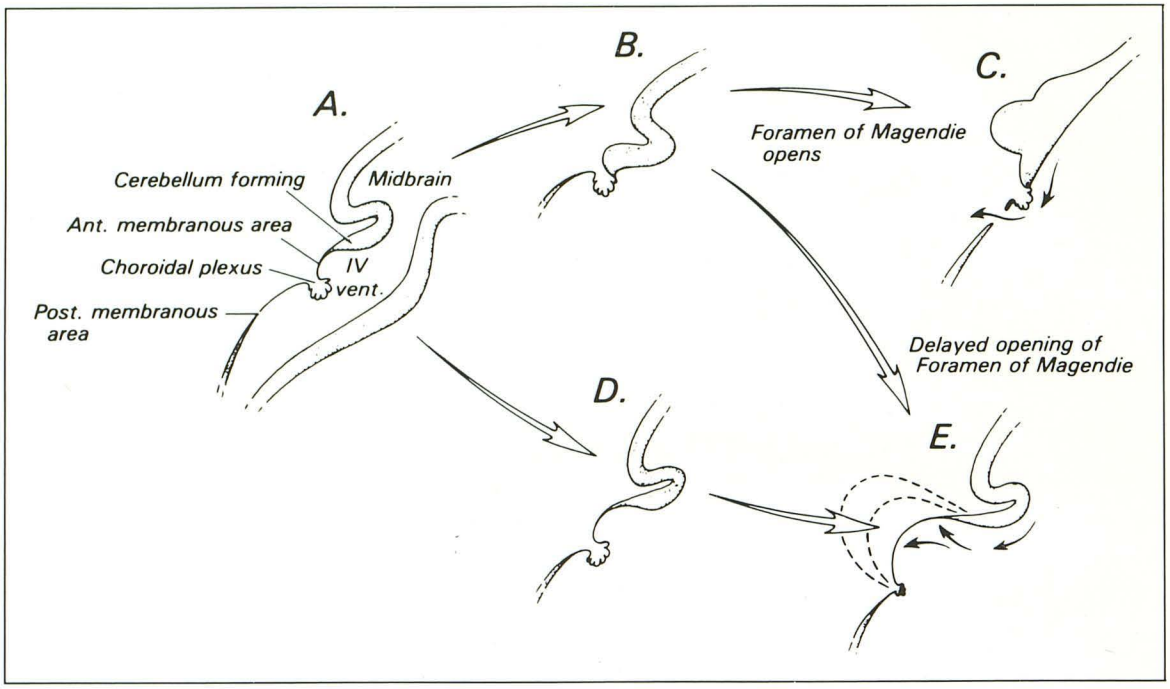


Fig. 7. Embryology; diagrammatic representation of the developing choroid plexus and roof of the fourth ventricle. Midsagittal section, cephalic is to the readers right.

*A*,–*C*, In the normal brain, the area membranacea superior (labeled *Ant. membranous area*) becomes incorporated into the developing choroid plexus, so the choroid comes to lie at the caudal edge of the cerebellum. The area membranacea inferior (labeled *Post, membranous area*) will be the site of the foramen of Magendie.

*D* and *E*, Failure to incorporate the area membranacea superior into the choroid plexus could lead to progressive ballooning of a thin-walled fourth ventricular cyst caudal to the vermis and cerebellum, but cephalic to the choroid plexus. This is the proposed embryogenesis of the Dandy-Walker malformation.

### *Dandy-Walker Malformation*

The Dandy-Walker malformation was first reported by Dandy and Blackfan (1914) who described marked dilatation of the fourth ventricle and anterior displacement of the vermis, which they attributed to primary atresia of the cerebellar foramina (22). A further review by Taggart and Walker (1942) (23) led Benda (1954) to suggest the name Dandy-Walker malformation (24). Benda emphasized that atresia of the outlet foramina of the fourth ventricle was not essential to this malformation.

The typical Dandy-Walker malformation is characterized by a triad of 1) complete or partial agenesis of the vermis, 2) cystic dilatation of the fourth ventricle, and 3) an enlarged posterior fossa with upward displacement of the lateral sinuses, tentorium, and torcular (Figs. 8–10) (2).

### *Clinical Findings*

The Dandy-Walker malformation occurs in 1 per 25,000–30,000 births (25). There is a slight, statistically insignificant, female predilection (25). Dandy-Walker malformation accounts for 2%–4% of hydrocephalus and 14% of cystic posterior fossa malformations (26). The disorder most commonly is an isolated malformation with a low risk of recurrence in later siblings (1%–5%) (27). However, the risk of recurrence may be high when the Dandy-Walker malformation is associated with 1) autosomal recessive Mendelian conditions such as Warburg syndrome, Coffin-Siris syndrome, Frasier cryptophthalmus and Meckel-Gruber syndrome; 2) the dominant X-linked Acardi syndrome; or 3) diverse chromosomal anomalies such as duplications of 5p, 8p, and 8q; trisomy of chromosomes 9, 13, and 18; and triploidy (27). Rubella, cytomegalovirus, toxoplasmosis, coumadin, and alcohol have also been reported to cause Dandy-Walker malformation.

Many Dandy-Walker patients show developmental delay. However, the degree of intellectual impairment may have been overestimated in the past. Hirsch et al found an intelligence quotient greater than 80 in 60% of patients (25). Golden et al found normal mental development in 75% of patients (28). Specific review of intellectual/motor outcome of 19 cases of Dandy-Walker


A B

C

Fig. 8. Comparison of normal brain and Dandy-Walker malformation.

*A*, Normal brain, midsagittal section, displays the expected shapes and relationships of the third ventricle (*3*), aqueduct (*black arrow*) and fourth ventricle (*4*), vermis and cerebellar hemisphere, falx, tentorium, inferior sagittal sinus (*arrowhead*), vein of Galen (*single white arrow*), and straight sinus (*double white arrow*). Note the branching pattern of the arbor vitae, the size and configuration of the brain stem and the contour of the midline posterior fossa (*dashed lines*).

*B*, Dandy-Walker malformation, midsagittal section, displays the anterosuperior displacement and counterclockwise rotation of the vermis (*V*) above the collicular plate, exposing the medial aspect of the cerebellar hemisphere (*H*), the huge fourth ventricular cyst (*white arrowheads*), the third ventricle (*3*), marked hydrocephalus with secondary deformity of the corpus callosum, abnormal elongation and elevation of the vein of Galen (*single white arrow*), and abnormal (fetal) position of the confluence (*double white arrows*) of the falx and tentorium. The aqueduct was patent but is sectioned here just lateral to its lumen.

*C*, Magnified view of the hindbrain. The branching pattern of the arbor vitae shows that many of the verminal lobules are intact, but hypoplastic. The anterior lobe is intact. The posterior lobe is intact, at least to pyramis. The tissue that should have formed the uvula and nodulus appears to form a thin band of distorted folia (*white arrowheads*) along the everting margin of the cyst (see also Fig. 10B).

(Figs. *B* and *C* reprinted with permission from Masdeu et al (67), through the kindness of Dr Joseph C. Masdeu, New York.)

syndrome documents that 47% have normal intellect with little or no motor deficit; an additional 26% have normal intellect and little to no motor deficit but require special help with specific learning disabilities; 11% have moderate developmental delay with little to no motor deficit; and 16% have severe delay with spastic cerebral palsy (29).

Greater than 80% of Dandy-Walker patients present with hydrocephalus early in life (2). However, the hydrocephalus is often *not* evident at birth; it develops postnatally and presents by 3 months of age in 75% of patients. This delay of onset of hydrocephalus may be explained by the secondary opening of the foramina of Luschka that occurs later, or by bleeding from unsupported, easily torn vessels along the wall of the large posterior fossa cyst at the time of delivery. The possibility that this bleeding may occur during labor lends support to those advocating Caesarian section for Dandy-Walker patients diagnosed prenatally (25).

These patients usually require surgery for correction of hydrocephalus. Cystoperitoneal and/or ventriculoperitoneal shunting are now the procedures of choice, although controversy persists as to which to perform first (30). Overall surgical mortality remains high: 12.5% (25). This mortal-

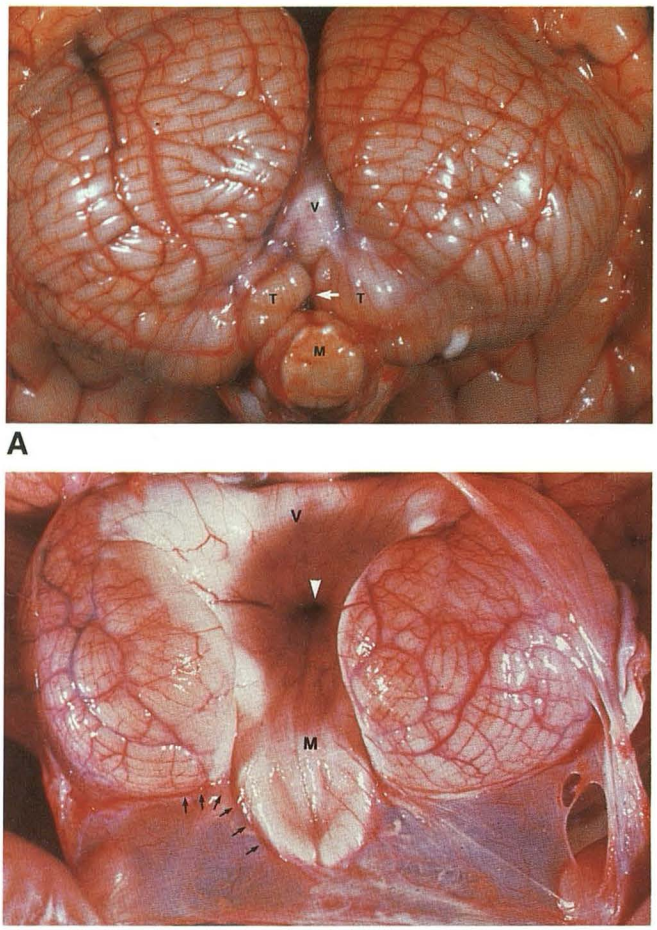


Fig. 9. Comparison of normal brain and Dandy-Walker malformation.

*A*, Normal unfixed cerebellum viewed from behind and below displays the folia and fissures of the hemispheres, the inferior vermis (*V*), the tonsils (*T*), and the medulla (*M*). The vallecula (*white arrow*) leads between the tonsils to the fourth ventricle (covered by the inferior vermis).

*B*, Dandy-Walker malformation. Unfixed specimen viewed from behind and below. The cerebellar hemispheres are hypoplastic and rotated laterally. The vermis is hypoplastic and rotated anterosuperiorly. The thin-walled fourth ventricular cyst attaches to the brain stem along the tela choroidea and expands behind and above the cerebellar hemispheres where it appears to attach along the posterolateral margin of the hemispheres (but see Fig. 13B). Consequently, one can look directly from the cyst through the fourth ventricle to the ventricular surface of the superior vermis (*V*), the ventricular end of the aqueduct (*white arrowhead*), and the ventricular surface of the medulla (*M*).

ity may result from upward herniation of the posterior fossa cyst following lateral ventriculoperitoneal shunting or downward herniation of the cerebrum and lateral ventricles following direct shunting of the cyst itself.

Concurrent systemic anomalies are present in approximately 25% of cases, and include low-set ears, polydactyly, syndactyly, Klippel-Feil syndrome, Cornelia de Lange syndrome, and cleft palate (Fig. 11) (2, 31). Facial angiomas are seen in approximately 10% of patients (25). Golden et al (31) observed two dissimilar populations with Dandy-Walker syndrome. Those with concurrent hydrocephalus had a very high incidence of other central nervous system (CNS) malformations (91%) and a smaller incidence of visceral anomalies (55%), including one case of secundum atrial septal defect (9%). Those without hydrocephalus had a very high incidence of complex cardiac malformations (80%).

### *Pathologic Changes*

**Bone and Dura:** The head circumference is increased with a dolichocephalic configuration (Fig. 11A). The lambdoid sutures may be widened and separated preferentially. The posterior fossa is markedly expanded (Fig. 11B). Cerebrospinal fluid (CSF) pulsations and secondary pressure changes cause erosive scalloping of the posterior surfaces of the petrous pyramids and of the occipital squama. Infrequently, marked expansion of the posterior fontanelle or a true dehiscence of the occipital squama is associated with an occipital encephalocele (32, 33). The tentorium and transverse sinuses lie in high position along the parietal bone (Fig. 8B) (34, 35). The incisura is inclined vertically and is wider than normal. The angle formed by the junction of the straight sinus with the superior sagittal sinus increases from a normal acute angle of 50°–75° to an obtuse angle of approximately 90°–150° (18). The falx cerebri is normal. There is no falx cerebelli in the true Dandy-Walker malformation (26).

**Cerebellum, Vermis and Brain Stem:** The vermis shows a range of deformity (Figs. 11 and 12). It is completely absent in approximately 25% of cases (2). The remainder show partial aplasia of the posterior vermis (2). The superior medullary velum and any residual portion of the superior vermis are rotated anterosuperiorly and reflected upward. In severe cases, they appear to be refolded up and over the quadrigeminal plate. The residual vermis may become attached to the tentorium. The inferior vermis is absent. The posterior medullary velum is rotated superiorly. The cerebellar hemispheres are hypoplastic (Figs.

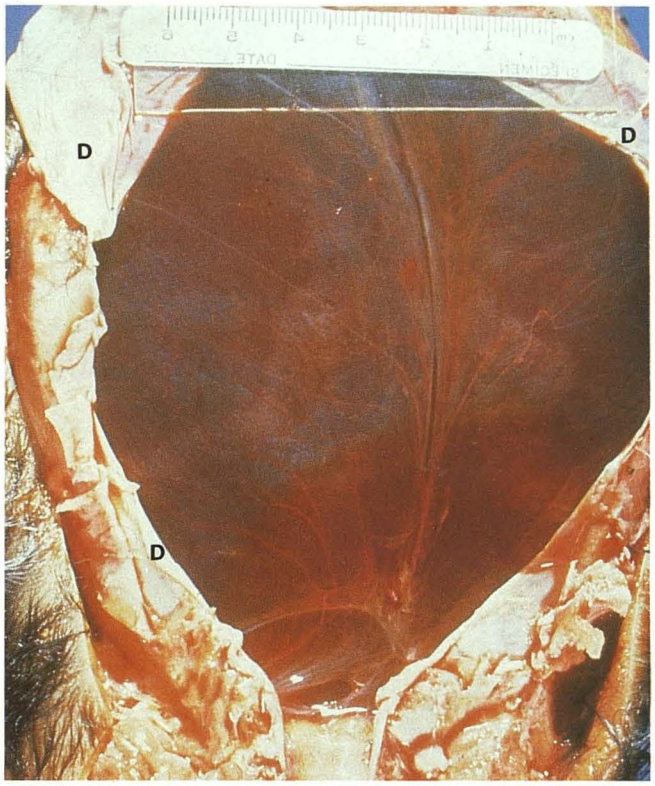


A

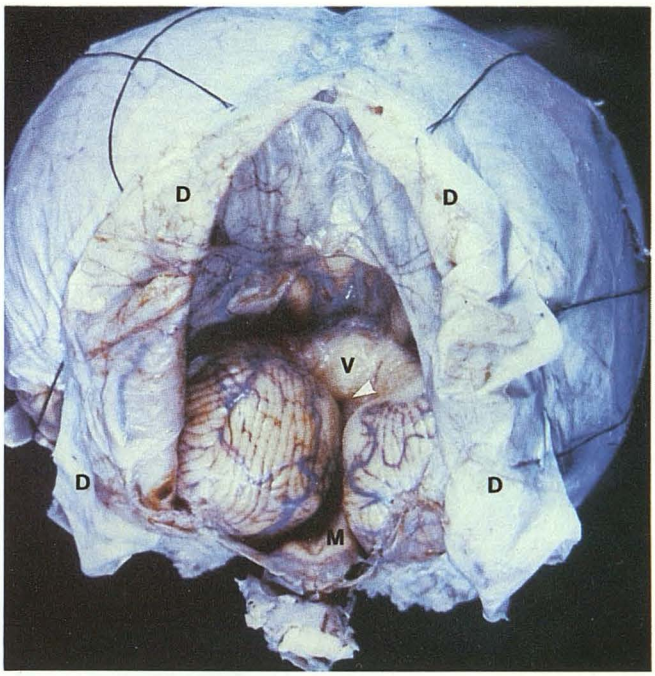


B

Fig. 10. Dandy-Walker malformation; two specimens.

*A*, View from behind. Opening and reflecting the dura (*D*) exposes the thin arachnoid external to the unruptured Dandy-Walker cyst.

*B*, Fixed specimen opening and reflecting the dura (*D*), arachnoid and cyst reveal the size of the cyst and its relationship to the cerebellum (same specimen as Figs. 8B and 8C). In this case, the hemispheres lie more closely together but remain ununited. The undersurface of vermis (*V*), aqueduct (*white arrowhead*) and floor of medulla (*M*) are visible through the midline defect. Note the vertical orientation of the incisura.

(Reprinted with permission from Masdeu et al (67), through the kindness of Dr Joseph C. Masdeu, New York.)

9 and 13). They appear to be "winged outward" and displaced anterolaterally against the petrous pyramids. They may be symmetrical or asymmetrical in size and position (35). There may be disorganization and heterotopias of the cerebellar cortex (2, 31). The brain stem usually appears small as a result of hypoplasia and of compression by the Dandy-Walker cyst. There can be pontine hypoplasia, subtotal aplasia of the inferior olives, and dysplasias of the other nuclear groups. Heterotopias of the inferior olivary nuclei and anomalies of the crossing corticospinal tracts are common (2). The aqueduct may be patent, narrowed, kinked, or occluded.

**Dandy-Walker Cyst:** The Dandy-Walker cyst is actually the distended fourth ventricle that balloons posteriorly behind the developing cerebellar hemispheres and displaces them laterally and anteriorly (Fig. 9). Conceptually, the cyst wall is formed of three layers (35). The inner layer is ependyma, which is continuous with the ependyma lining the wall of the anterior fourth ventricle. This layer may show discontinuities where the ependyma is reduced to small ependymal nests (2). The outer layer is pia, which is reflected around the cyst to be continuous with the pia along the medial and posterior surfaces of the cerebellar hemispheres. The intermediate layer is the stretched out neuroglial tissue that would have formed the inferior vermis and medial hemispheres. This residual tissue is thickest laterally and superiorly, near to the hemispheres, tonsils, and residual superior vermis. Calcification may be present in this tissue (7%) (31).

The cyst wall is attenuated progressively toward the midline where the fourth ventricle expanded most widely. Thus, the anterolateral walls of the fourth ventricle-cyst are the smooth white matter of the residual vermis and the cerebellar hemispheres (2) (Figs. 9B and 13). The posterior wall of the fourth ventricle-cyst is a thin, easily ruptured, translucent membrane (2). The cyst wall attaches to the brain stem along the course of the tela choroidea. It *appears* to be attached to the cerebellar hemispheres posterolaterally, but the reflection of the cyst can often be traced

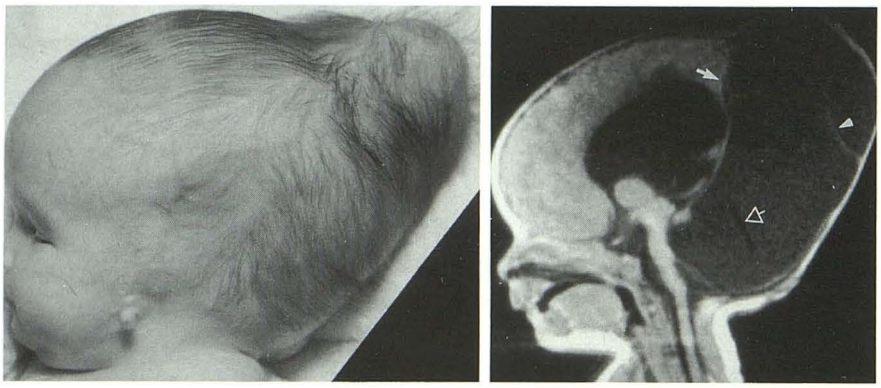


Fig. 11. Dandy-Walker malformation, 1 month-old girl.

*A*, Lateral patient photograph shows marked dolichocephaly, bulging posterior fontanelle, low-set malformed pinna and atresia of the external auditory canal.

*B*, Midsagittal T1 MR reveals that the dolichocephaly and bulging fontanelle result directly from the gross expansion of the posterior fossa cyst. The tentorium and straight sinus (*closed white arrow*) are elevated so the bulging fontanelle is purely infratentorial. The superior vermis is tiny. The brain stem is hypoplastic. The cyst membrane (*white arrowhead*) has partially collapsed away from the dural wall of the posterior fossa after shunting. Note flow void (*open white arrow*) in shunt.

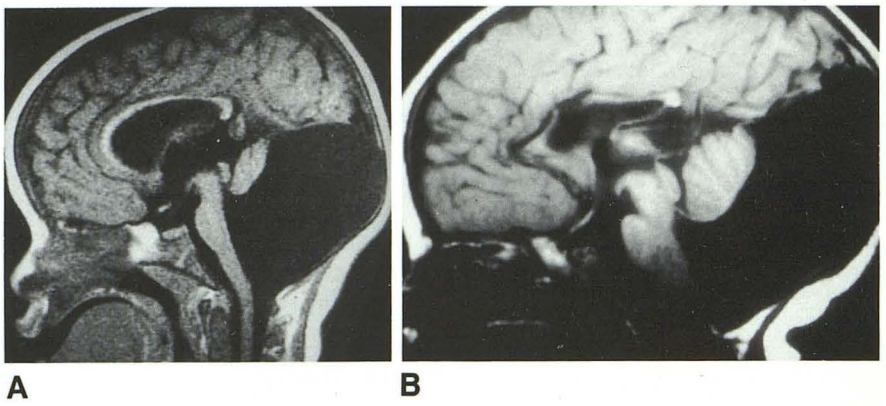


Fig. 12. Dandy-Walker malformation. *A–B*, Midsagittal T1 MR from two patients shows that the vermis is hypoplastic and rotated anterosuperiorly by the cyst in each case. Together with Figure 11B, these figures show a gradation of vermian hypoplasia.

far medially to where it joins the white matter of the fourth ventricle.

The choroid plexus is displaced far laterally and inferiorly, and comes to lie within the lateral recesses and along the caudal insertion of the cyst wall at the medulla (2). Choroid plexus may be entirely absent from the fourth ventricle at postmortem in 40% of cases (36). The exit foramina of the fourth ventricle may be patent or occluded. Hart et al documented patency of the foramen of Magendie at postmortem in at least two of their 28 cases of Dandy-Walker malformation (7%) and patency of the foramina of Luschka in 18% (31). The foramina were clearly closed in 18%. Hirsch et al showed communication between the fourth ventricle and the subarachnoid space in vivo in more than 80% of cases (25).

Between the outer pia of the cyst wall and the pia of the cerebellar hemispheres is a thin compressed subarachnoid space (Fig. 13) (35). External to that is the normal arachnoid mater of the cisterna magna, the dura that lines the inner table of the occipital bone, and the inner table itself. The expanding cyst bulges into, expands, and occupies the space that would have become cisterna magna. The outer cyst wall bulges against the midline arachnoid so tightly it almost "closes" the space. The "normal" subarachnoid space between the Dandy-Walker cyst and the occipital bone becomes visible only when shunting of the cyst collapses the cyst wall away from the occipital bone (Fig. 13), or when contrast is introduced into the subarachnoid space (Fig. 14).

The cyst occupies most of the enlarged posterior fossa. In 44% of cases, the cyst has a superior extension or diverticulum that extends superior to the residual superior vermis. This may bulge into the quadrigeminal plate cistern above the tentorium (37). The superior extension of the cyst

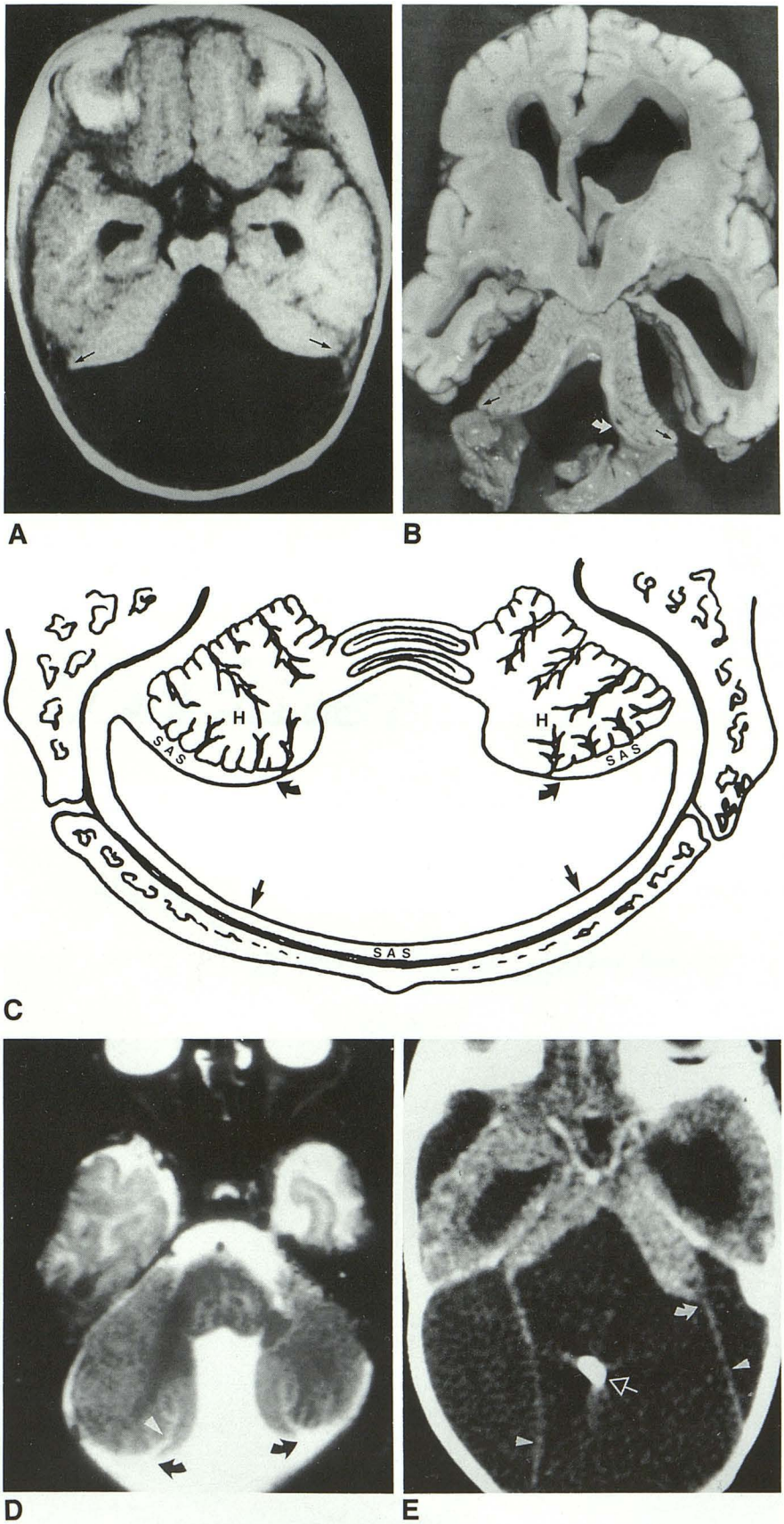


Fig. 13. Dandy-Walker malformation; relationship of the cerebellar hemispheres and the fourth ventricular cyst.

*A*, Untreated Dandy-Walker malformation, Axial T1 MR. The cerebellar hemispheres are hypoplastic and winged anterolaterally by expansion of the cyst posteriorly. No space is seen between the cyst and the cerebellum or between the cyst and the wall of the posterior fossa. Note that the cyst stops exactly at the lateral angle of the cerebellar hemispheres (*arrows*) and does not extend anterior to them.

*B*, Shunted Dandy-Walker malformation with intraventricular hemorrhage. Postmortem specimen; 3-month-old girl. The cyst wall (*curved arrow*) appears to arise in continuity with the white matter of the cerebellar hemispheres and to extend posterolaterally behind—but separate from—the posterior surface of the cerebellar hemispheres to the lateral angle of the hemispheres (*black arrows*). It is then reflected posteromedially to form the back wall of the cyst.

*C*, Diagrammatic representation of the Dandy-Walker cyst arising (*curved black arrows*) medially from the white matter of the cerebellar hemispheres and forming a wall (*black arrows*) that is interposed between the cerebellar hemispheres (*H*) and the bony posterior fossa, but remains separate from them. The pial lining of the dorsal surface of the hemispheres is reflected into the anterolateral portion of the cyst wall leaving a compressed subarachnoid space between the cyst and the hemispheres and between the cyst and the dorsal dura.

*D*, Shunted Dandy-Walker cyst, T2 MR. Note the fluid in the subarachnoid space (*white arrowhead*) between the dorsal surface of the cerebellar hemispheres and the origin (*curved black arrows*) of the cyst along the side wall of the fourth ventricle.

*E*, Shunted Dandy-Walker malformation (same patient as Fig. 11). Contrast-enhanced CT shows the expanded posterior fossa and enhancing tentorium. Shunt (*open white arrow*) decompression collapses the cyst wall (*white arrowheads*), separating it from the bony and dural walls of the posterior fossa and from the posterior surface of the cerebellar hemispheres (*H*, *H*). Compare the origins (*curved white arrow*) of the cyst wall in *B*, *C*, *D*, and *E*.

does not communicate with the quadrigeminal cistern or the suprapineal recess but may compress these structures. Inferiorly, the cyst usually extends downward through the foramen magnum behind the cord to the C1-C2 level. In the untreated state (Fig. 13A) the cyst does not extend anterior to the cerebellar hemispheres, ie, anterior to the lateral angles of the cerebellum (between the anterior cerebellum and the petrous pyramid) (35). If a cyst extends anterior to the lateral angle of the cerebellum in the untreated case, the cyst most likely represents an arachnoid cyst, not the cyst of a Dandy-Walker malformation (Dr Larissa Bilaniuk, Philadelphia, unpublished data) (see Fig. 22).

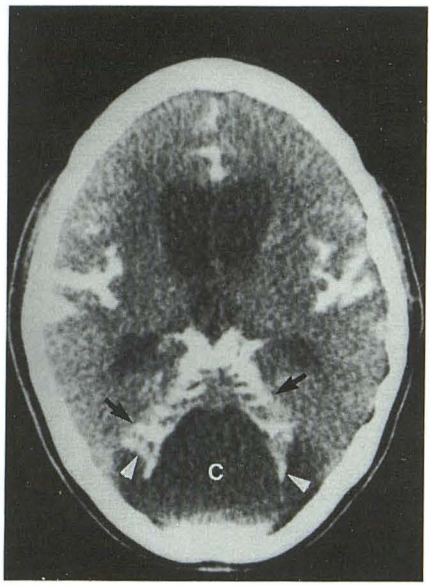


Fig. 14. Dandy-Walker malformation; axial CT. Contrast placed into the lumbar subarachnoid space and carried cranially delineates the supratentorial cisterns, the cisterns along the cerebellar hemispheres (*black arrows*), and the thin subarachnoid cisterns (*white arrowheads*) between the cyst (*C*) and the dorsal surface of the cerebellar hemispheres. Contrast also layers posteriorly against the occipital squama. (Case courtesy of Dr Jeremy Altman; reprinted with permission from Naidich et al (35).)

**Ventricles:** Patients with Dandy-Walker malformation almost always develop hydrocephalus (Fig. 8B). The degree of hydrocephalus varies from mild to severe and does not correlate with the size of the posterior fossa. The site of CSF obstruction varies: Carmel et al (36) found aqueductal stenosis in 28% of cases, communication between the third ventricle and the cyst in 72% of cases, patency of the fourth ventricular foramina in 39% of cases, and obstruction of the incisura in 11% of cases. When the aqueduct is occluded, shunting the lateral ventricles may cause upward herniation of the undecompressed fourth ventricular cyst and a characteristic "snow man" deformity of the posterior fossa cyst (Fig. 15). Conversely, direct shunting of the noncommunicating fourth ventricular cyst may cause downward transincisural herniation of the undecompressed lateral ventricles (38). In such a case, the portion herniating is usually the medial atrial

Fig. 15. Dandy-Walker malformation; upward herniation following direct shunting of the lateral ventricle only. Axial CT after instillation of contrast via the ventricular catheter show decompression of the lateral ventricular hydrocephalus with marked upward herniation of the noncommunicating, undecompressed Dandy-Walker cyst. Note the mild constriction (*arrows*) of the cyst by the tentorium at the wide incisura.

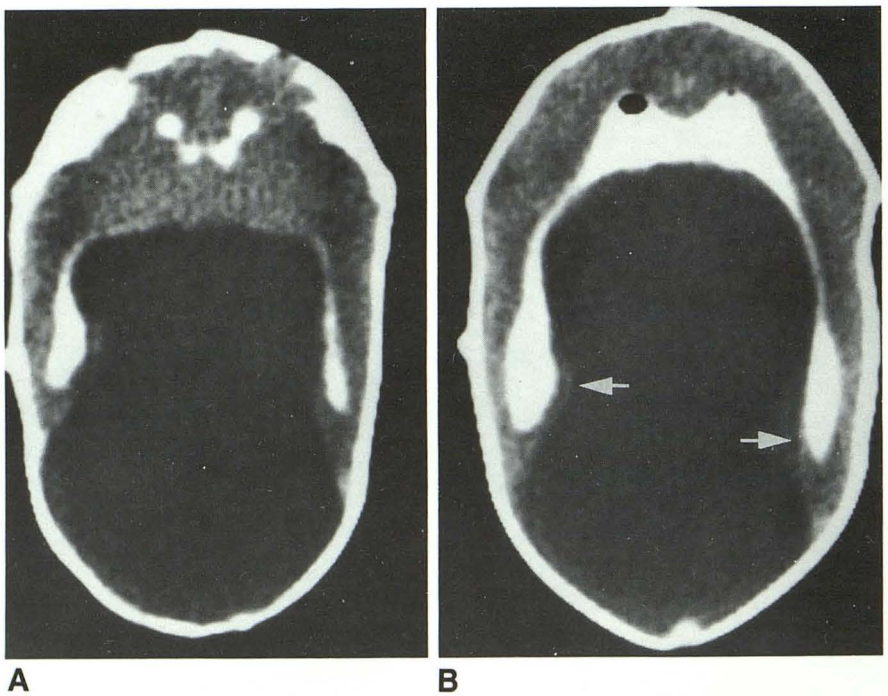

wall, forming diverticula that extend into the posterior fossa unilaterally or bilaterally. Approximately 25% of Dandy-Walker patients show downward herniation of the medial atrial walls after shunt therapy (Fig. 16). This post-shunting herniation results from a transincisural pressure gradient caused by malfunction of a ventriculoperitoneal shunt, application of suction to the cystoperitoneal shunt, or increase in supratentorial pressure for unknown causes (38). Once the herniation occurs, it may persist despite shunt revision and restoration of normal pressure gradients (38).

The patency of the CSF pathways is important to determine in Dandy-Walker malformation. Magnetic resonance (MR) demonstration of CSF flow may obviate the need for ventriculography, direct opacification of the cyst, or placement of contrast into the subarachnoid space before therapy with diverting shunts. Contrast placed into the subarachnoid space fills the compressed cisterna magna and percolates into the small subarachnoid space between the cyst wall and the posterior surface of the cerebellar hemispheres (35). If the foramen of Luschka is patent, contrast may also enter the cyst itself.

**Vasculature:** The anomalies of the vertebral basilar vasculature associated with Dandy-Walker malformation have been described by Wolpert et al and by La Torre and associates (39, 40). Patients with the Dandy-Walker malformation demonstrate high position of the posterior cerebral vessels due to the high tentorium. The superior cerebellar arteries are often displaced anterosuperiorly, above the posterior cerebral arteries, due to the marked enlargement of the fourth ventricle. The posterior-inferior cerebellar arteries are shortened with superior displacement of the tonsilar loops (35). The inferior vermian branches are often lacking. The venous phase show absent

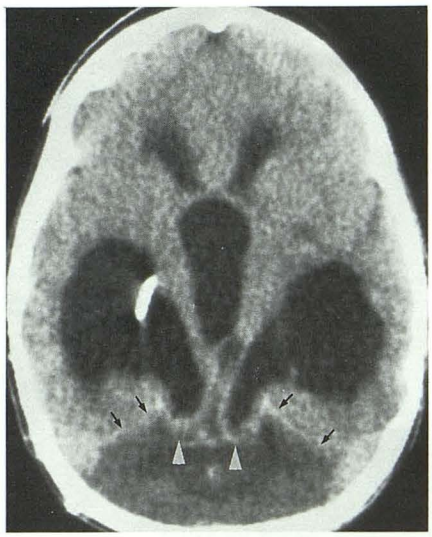

A

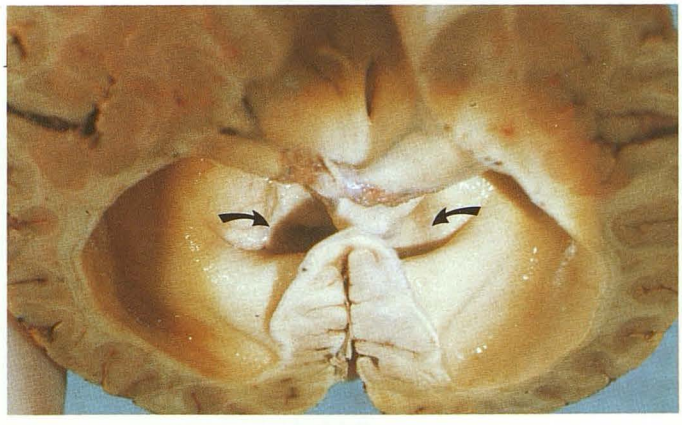

B

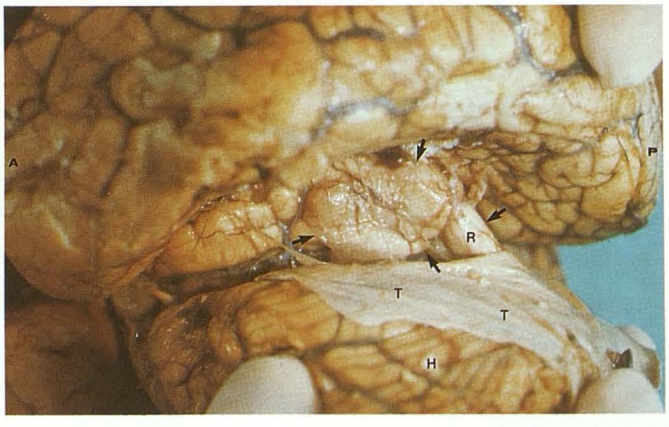


C

Fig. 16. Dandy-Walker malformation; downward transincisural herniation post-shunting; 4 ½-year-old boy.

*A*, Axial CT following multiple shunt revisions for shunt malfunction show the decompressed posterior fossa, persistent dilatation of the lateral and third ventricles despite the lateral ventricular shunt, and bilateral medial atrial diverticula (*white arrowheads*) that herniate downward through the incisura of the tentorium (*arrowheads*).

*B* and *C*, Postmortem specimen, same patient.

*B*, Axial section through the lateral ventricle shows atrial dilatation and the ostia of the bilateral atrial diverticula (*curved arrows*).

*C*, Lateral view of the cerebrum (*A* = anterior, *P* = posterior), the tentorium (*T*) and the cerebellar hemisphere (*H*) shows the two left (*L*) and right (*R*) medial atrial diverticula (*arrows*) that herniated downward *through* the incisura before the cerebrum was lifted upward to obtain this picture. (*C* reprinted with permission from Naidich et al (38).)

inferior vermian vein, elevation of the great vein of Galen, and high position of the transverse sinuses and torcular. Arachnoid cysts, in contradistinction, show a normal complement of vessels that are secondarily displaced and compressed by the avascular retrocerebellar cyst (39, 40).

**Associated CNS Anomalies:** The Dandy-Walker malformation is associated with other CNS abnormalities in 68% of cases (30). These include supratentorial abnormalities such as callosal dysgenesis (one-sixth of patients), subependymal neuronal heterotopias polymicrogyria, agyria, schizencephaly, and lipomas (Fig. 17). Of these, the callosal dysgenesis is the most frequently associated supratentorial abnormality (31). Encephaloceles and lumbosacral meningocele may also concur.

## Dandy-Walker Variant

The Dandy-Walker variant consists of hypoplasia of the cerebellar vermis with cystic dilatation of the fourth ventricle, but no enlargement of the posterior fossa (41). Hydrocephalus may be present or not.

Clinically, these children may present with an enlarging head due to hydrocephalus or with developmental delay. The Dandy-Walker variant is more common than the true Dandy-Walker malformation and accounts for one third of posterior fossa malformations (26). Shunting is performed only if there is hydrocephalus. The supratentorial anomalies associated with Dandy-Walker variant include agenesis of the corpus callosum (21%), malformations of cerebral gyri and cerebral heterotopias (21%), holoprosen-

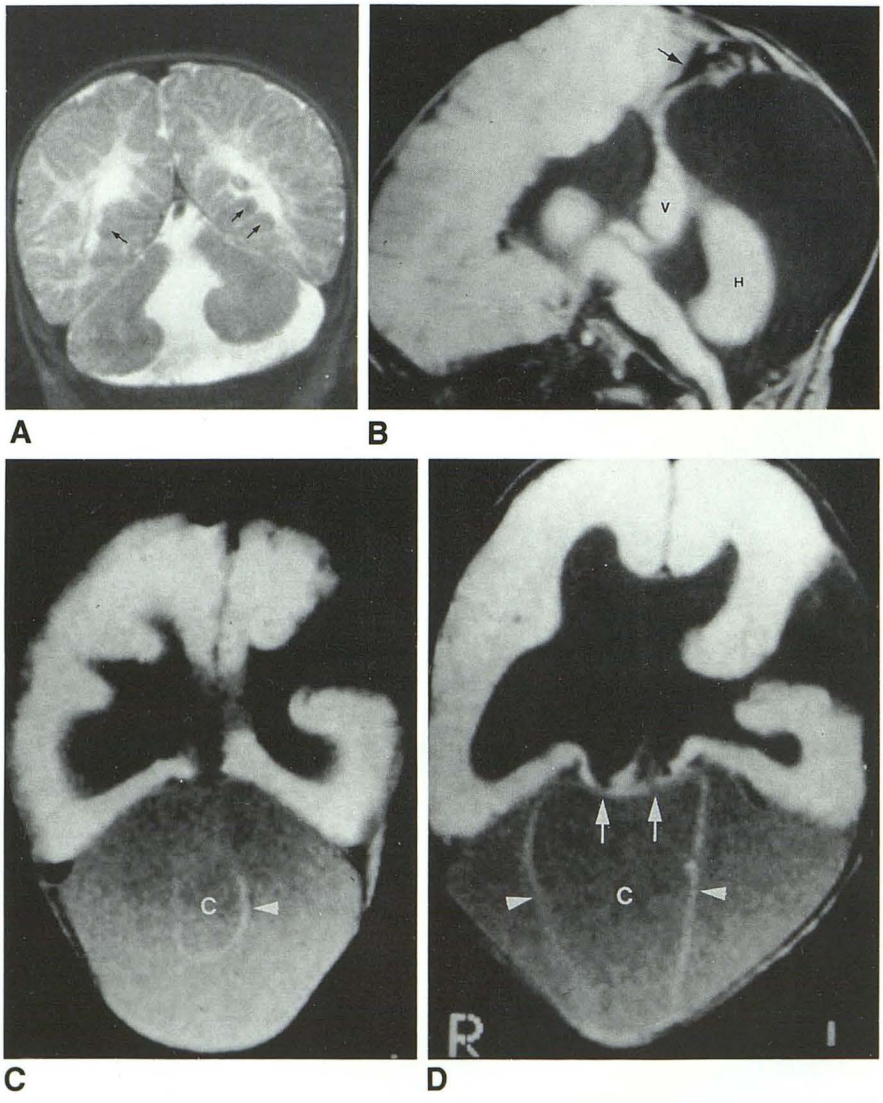


Fig. 17. Dandy-Walker malformation; concurrent CNS anomalies.

*A*, Neuronal heterotopia. Coronal T2 MR shows subependymal nodules of heterotopic gray matter (*arrows*) with Dandy-Walker malformation.

*B*, Callosal agenesis. Sagittal T1 MR. Note the position of the straight sinus (*arrow*) at the vertex. *V* = vermis; *H* = cerebellar hemisphere.

*C* and *D*, Axial proton density MR show bilateral schizencephaly, agyria/pachygyria, absent septum pellucidum, and callosal dysgenesis with collapse of the Dandy-Walker cyst (*C*) wall (*arrowheads*) and bilateral medial atrial diverticula (*white arrows*) following shunt decompression of the cyst (same patient as Fig. 11 and Fig. 13E.)

cephaly (10%), diencephalic cysts (10%), and posterior fossa meningoencephalocele (10%) (26). Mental deficiency appears to be related to the associated supratentorial anomalies.

Pathologically, the fourth ventricle is large but less dilated and better formed than in true Dandy-Walker malformation (Fig. 18) (35). The tentorium is high in only 10% of cases. There is a falx cerebelli in 32% of cases, although it may be displaced (35). There is less severe hypoplasia of the inferior vermis and less severe superoanterior rotation of the superior vermis. The cerebellar hemispheres are hypoplastic. The brain stem usually appears nearly normal (Fig. 19). Rarely, dermal sinuses and teratoma may concur (Fig. 20).

## Mega Cisterna Magna

The term mega cisterna magna (synonyms: retrocerebellar arachnoid pouch, communicating arachnoid cyst, and Blake pouch cyst) refers to a cystic malformation of the posterior fossa characterized by an intact vermis, an enlarged cisterna magna, and an enlarged bony/dural posterior fossa. The size of the mega cisterna magna is variable. The fourth ventricle communicates with the subarachnoid space (Fig. 21). The brain stem and the cerebellum are usually normal. This condition accounts for 54% of the cystic posterior fossa malformations (26).

Clinically, these children present with hydrocephalus and/or developmental delay. The mental retardation is due to associated supratentorial anomalies, such as agenesis of the corpus callosum (6%), diencephalic cysts (6%), and holoprosencephaly (6%) (26). Posterior meningoceles are identified in 3% of cases (26). Rarely, there is neuronal heterotopia supratentorially. Posterior meningoceles are also identified in 3% of cases (26).

Pathologically, there is evagination of the tela choroidea of the fourth ventricle behind the intact vermis and cerebellar hemispheres. The cystic expansion of the tela choroidea may extend far beyond the normal borders of the cisterna magna laterally, posteriorly, and superiorly (35). It may reach the quadrigeminal plate cistern but does not communicate with it (Fig. 21). The cyst may extend superiorly into a focal dehiscence of the falcotentorial junction and, then, is usually associated with an interruption or fenestration of the straight sinus. The tentorium is elevated in 12.5% of cases. A falx cerebelli is seen in 62.5% of cases (35). The brain stem is typically normal (18).

## Embryogenesis of the Dandy-Walker Complex

Embryologically, the Dandy-Walker malformation is believed to result from a broad insult to the alar plate involving the dorsal fourth ven-

A B

Fig. 18. Dandy-Walker variant; postmortem specimen. *A*, Midsagittal section, and *B*, posterior inferior view of the uncut specimen, show mild vermian hypoplasia and communication of the ventricle with the posterior fossa space medial to the cerebellar hemispheres through a large vallecula.

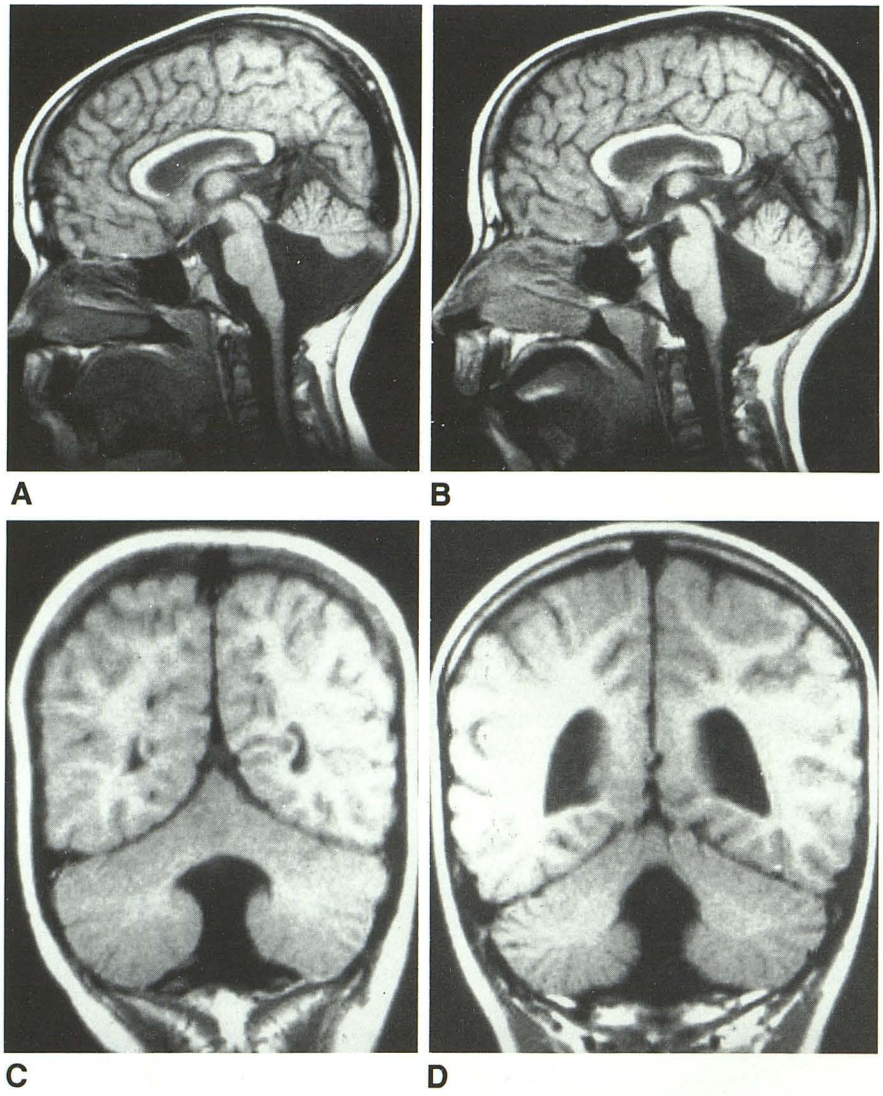


Fig. 19. Dandy-Walker variant; twin patients. *A* and *B*, Midsagittal T1 MR, *C* and *D*, corresponding coronal T1 MR. The twins show slightly different degrees of vermian hypoplasia and rotation and slightly different degrees of fourth ventricular dilatation. The cerebellar hemispheres are nearly normal. The posterior fossae are only slightly enlarged.

tricle and the rhombic lips (28). The manifestations of the Dandy-Walker malformation would appear to be explained best by failure to incorporate the area membranacea superior into the developing choroid plexus at the proper time (Fig. 7) (20). Persistence of this membrane between the caudal edge of the developing vermis and the rostral edge of the developing choroid plexus easily explain the large fourth ventricular (rhombencephalic) cyst that balloons posterior to the cerebellar hemispheres, the relation of the cyst to the vermian remnant anterosuperiorly, the insertion of the cyst into the brain stem along the tela choroidea (but insertion of the cyst into the white matter of the medial surfaces of the cerebellar hemispheres), and the low position of the choroid plexus. The area membranacea inferior could persist unopened leading to absence of the foramen of Magendie, or it could open at the appropriate or at a later time, accounting for the variability observed.

The high position of the tentorium, straight sinus, and torcular may indicate arrested development with the straight sinus remaining at the vertex as it is in the early embryo, with failure to migrate to its normal deep occipital position (1). Mechanical interference with such migration because of the expanding posterior fossa cyst may also contribute.

The variations in the severity of the malformation among the true Dandy-Walker, the Dandy-Walker variant, and the mega cisterna magna could be explained in terms of the severity of the initial insult leading to vermian hypoplasia and to persistence of the area membranacea superior. If the insult is sever and diffuse, it may affect the cerebellar hemispheres, vermis, and fourth ventricular roof leading to the classic

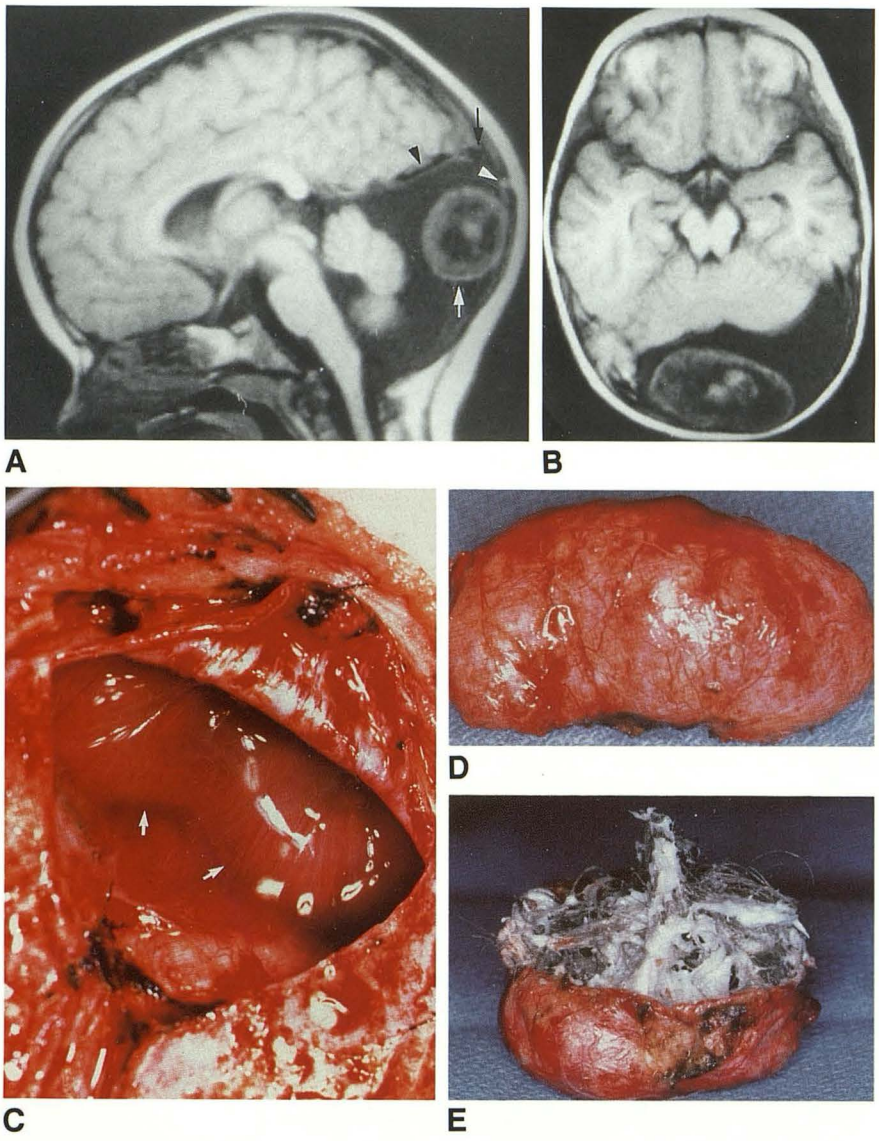


Fig. 20. Dandy-Walker variant with midoccipital dermal sinus and teratoma.

*A*, Midsagittal T1 MR shows vermian hypoplasia and rotation, enlarged fourth ventricle and retrocerebellar cyst, slightly high position of the straight sinus (*black arrowhead*) and torcular (*black arrow*), and an infratorcular sinus tract (*white arrowhead*) that leads to an ovoid mass (*white arrow*) within the retrocerebellar cyst.

*B*, Axial T1 MR through the upper cerebellum shows the transverse extent of the cyst and mass and the heterogeneous content of the mass.

*C–E*, Surgical photographs.

*C*, Operative exposure. After suboccipital craniotomy and opening of the dura, the mass (*arrows*) is seen to lie deep to the arachnoid.

*D*, External surface of mass.

*E*, Opening the mass reveals hair, cartilage, and sebaceous debris of a teratoma.

Dandy-Walker malformation (18). More localized insult to the developing cerebellum could lead to vermian/cerebellar hypoplasia with little effect on the fourth ventricular roof. This could result in the Dandy-Walker variant (18). Greater effect of the insult on the fourth ventricular roof than on the developing cerebellar primordia could lead to cystic dilatation of the ventricle and little cerebellar hypoplasia, as is seen with mega cisterna magna (18).

### Posterior Fossa Arachnoid Cyst

True arachnoid cysts are collections of CSF enclosed within the layers of the pia-arachnoid and lined by arachnoid cells and collagen (35).

Clinically, the arachnoid cysts present at varying ages from the first few months of life until adulthood. Most lesions appear to be sporadic, although arachnoid cyst may be associated with the mucopolysaccharides or with the conditions of dural ectasia such as neurofibromatosis.

The major clinical symptoms result from hydrocephalus and compression of the underlying brain (Fig. 22). Ataxia is frequent, headache and dysdiadochokinesia less common (18). In newborns, arachnoid cysts may present as rapid expansion of the cyst by hemorrhage due to the trauma of delivery and rupture of bridging veins (Fig. 23). Risk of such hemorrhage may indicate need for a Cesarean section if the diagnosis is made prenatally. No supratentorial anomalies or

systemic anomalies are specifically associated with the retrocerebellar arachnoid cyst.

Increasing use of neuroimaging has led to increased recognition of small, asymptomatic, apparently incidental posterior fossa cysts. Serial studies will determine whether a proportion of these ever becomes symptomatic. When there is hydrocephalus, these cysts may be decompressed successfully with either cystoperitoneal shunting or fenestration.

Pathologically, one-fourth to one-third of all arachnoid cysts involve the posterior fossa. Eleven percent are situated within the cerebellopontine angle, 10% lie in the quadrigeminal plate cistern, 9% are related to the vermis, and 3% lie in the prepontine and interpeduncular cisterns (35). The cysts may extend through the incisura or the foramen magnum.

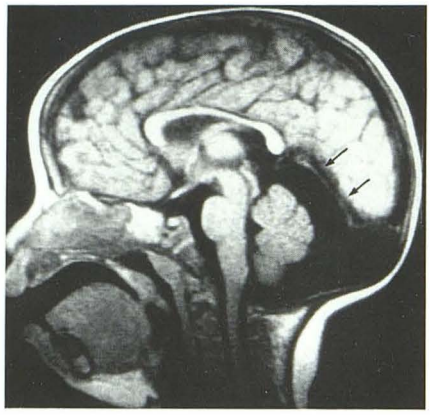

Fig. 21. Mega cisterna magna. Midsagittal T1 MR shows a normal vermis, fourth ventricle, and vallecula with a large cisterna magna that extends above the vermis toward the quadrigeminal plate cistern, and posterosuperiorly through a focal deficiency in the falx and tentorium, associated with a posterior fenestration of the straight sinus (*arrows*). The inner table of the occipital squama is scalloped.

The arachnoid cysts are unilocular, round, oval, or crescentic, fluid-filled masses that can be separated from the fourth ventricle and the vallecula (Fig. 22). The vermis, cerebellar hemispheres, and brain stem are normal except for associated mass effect. There are no mural nodules or calcifications. Ultrastructural studies have shown certain cells along the interior wall of the cyst contain specialized membranes and enzymes usually associated with secretory activity (42). It may be that CSF accumulates within the cyst as a result of secretion from these cells, rather than by osmotically induced filtration or a ball-valve mechanism (34).

Imaging studies show that the cyst fluid has computed tomography (CT) density or MR signal intensity nearly identical to the CSF of the ventricular system (35). There is no evidence of contrast enhancement. Many arachnoid cysts extend anterior to the cerebellar hemispheres (Fig. 23), so it is easy to rule out the Dandy-Walker complex. However, those arachnoid cysts that originate in the midline and lie wholly posterior to the cerebellum may be difficult to differentiate from the mega cisterna magna itself, except for their mass effect.

Embryologically, the retrocerebellar arachnoid cyst may represent a persistent diverticulum of the fourth ventricle, which fails to involute (the Blake pouch) (43). It may represent a focal failure

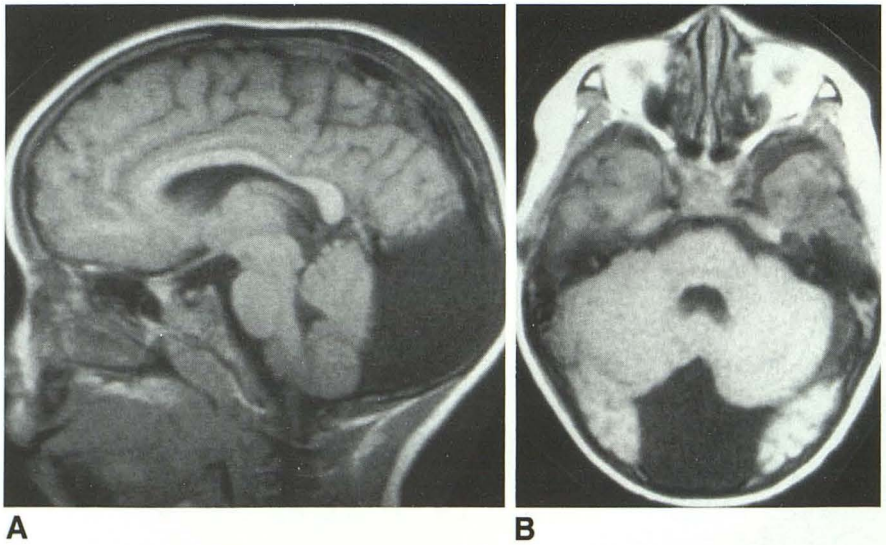


Fig. 22. Posterior fossa arachnoid cyst, sagittal (*A*) and axial (*B*) T1 MR images demonstrate a large posterior fossa CSF collection that compresses the vermis and displaces it anteriorly. The occipital bone shows slight scalloping. The straight sinus is slightly elevated. No communication with the fourth ventricle or vallecula is demonstrated. The cyst lies entirely within the midline.

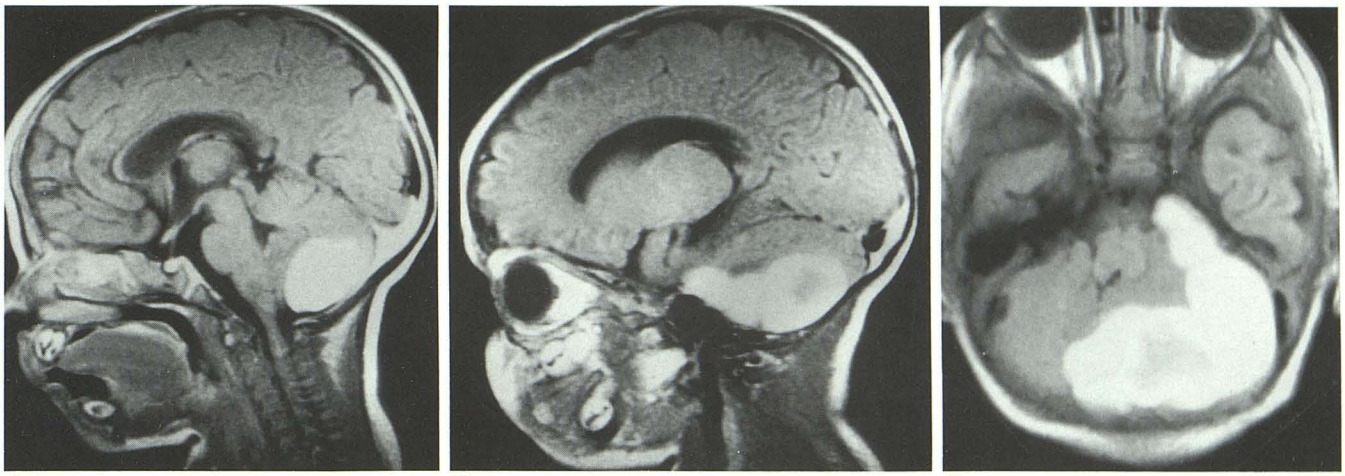


Fig. 23. Hemorrhagic posterior fossa arachnoid cyst. Midsagittal (*A*), left parasagittal (*B*), and axial (*C*) T1 MR images demonstrate a large asymmetric posterior fossa arachnoid cyst that extends from the posterior midline into the left cerebellar pontine angle anterior to the cerebellar hemisphere and compresses the neural structures. Increased signal intensity within the cyst represents methemoglobin. There is no hemorrhage within the ventricles or other sign of communication with the fourth ventricle.

to establish free communication throughout the developing space between the inner and the outer layers of the pia-arachnoid as the mesenchyme condenses (44).

### Joubert Syndrome

This familial syndrome was described by Joubert et al (1969) in four siblings, all of whom presented with neonatal hyperpnea alternating with apnea, abnormal eye movements, ataxia, and psychomotor retardation (45). Two of these children had agenesis of the posterior vermis, one had complete agenesis of the vermis at postmortem, and the fourth had complete agenesis of the vermis with an occipital meningoencephalocele (probably a gliocele) (45). The tentorium was elevated in three of the four siblings (45).

Joubert syndrome is inherited as an autosomal recessive trait, so genetic counseling of the parents is indicated. Males predominate by more than 2:1 (2). The children are mentally retarded, hypotonic, and ataxic with a poor clinical outcome. Hemifacial spasms, campylodactyly, syndactyly, and cystic kidneys also concur (45).

Joubert patients usually present as neonates with breathing abnormalities that improve with age. In Kendall's series, 44% of children had respiratory abnormalities (46). Visual difficulties are common. Sixty-seven percent of cases show nystagmus or abnormalities of supranuclear control of eye movements (46). Forty-four percent show mild to moderate reduction in visual acuity and retinal dystrophy (46). These clinical abnormalities can be related to dysfunction of the cerebellum and medulla oblongata. The episodic tachypnea and apnea are most likely due to abnormalities in the solitary fascicle and the nuclei gracili of the brain stem that control afferent respiratory impulses (42). The oculomotor dysfunctions such as dysmetric saccades, impairment of smooth pursuit, and optokinetic nystagmus can be related to abnormalities in the vermis. Decrease of the velocity of the saccadic eye movement may be associated with brain stem abnormalities (42).

Pathologically, Joubert patients show a variable degree of dysplasia of the cerebellar vermis (Figs. 24 and 25) (46, 47). The vermis may be completely absent or show partial agenesis/hypoplasia that affects either the superior or the inferior vermis predominantly (46). In Kendall's series, the posterior vermis was dysplastic in all cases and exhibited a deep midline groove or cleft (46). The superior vermis showed particular hypoplasia of the culmen (46). The inferior cerebellar peduncles were small (46). The superior cerebellar peduncles were small and appeared to course nearly perpendicular to the brain stem (46). The fourth ventricle was modestly enlarged but there was no hydrocephalus or posterior fossa cyst, so the posterior fossa was not expanded.

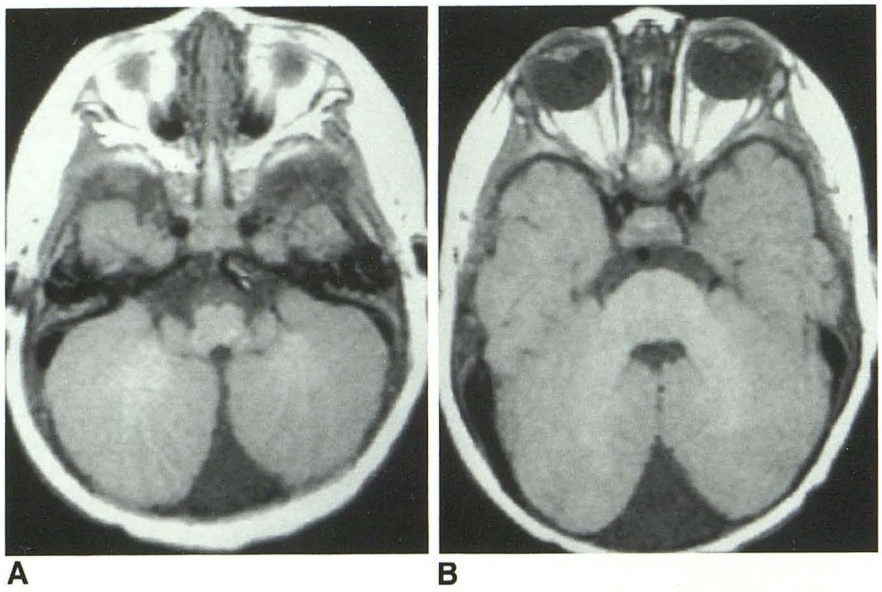


Fig. 24. Joubert syndrome. Axial T1 MR sections at the medulla (*A*) and the pons (*B*) show absence of the inferior vermis and thimble shape of the fourth ventricle. The fourth ventricle communicates directly with the enlarged cisterna magna.

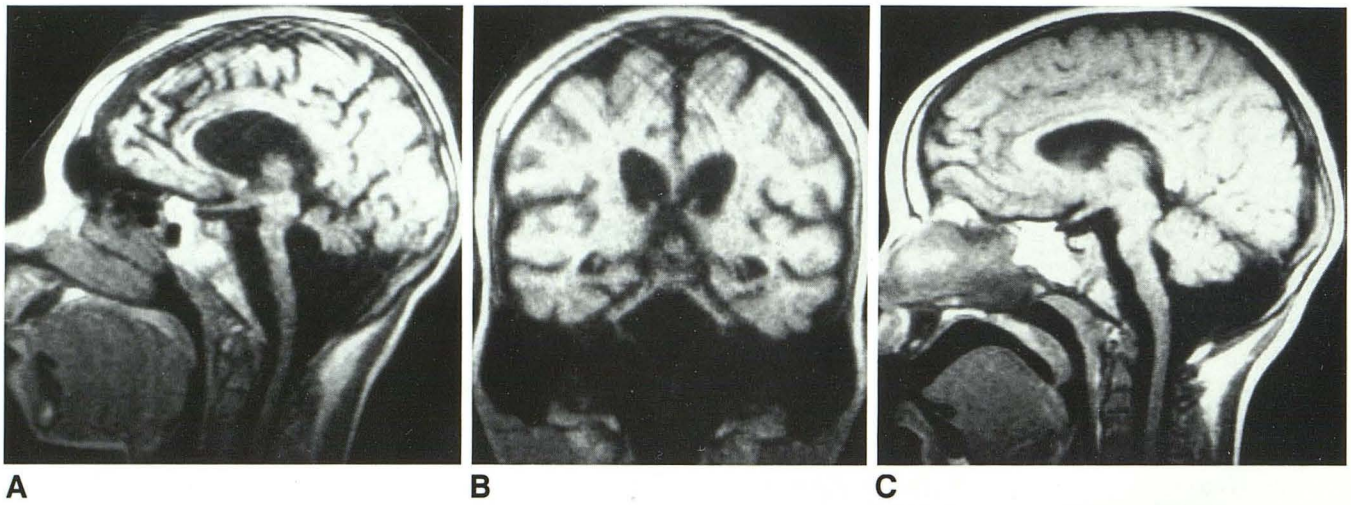


Fig. 25. Joubert syndrome in two siblings.

*A* and *B*, T1 MR images of the older child in the sagittal (*A*) and coronal (*B*) planes demonstrate marked vermian dysgenesis, hypoplasia of the cerebellar hemispheres, and hypoplasia of the brain stem. The basilar cisterns, fourth ventricle, and cisterna magna are enlarged secondarily. The posterior fossa is not enlarged. The cerebral hemispheres are atrophic.

*C* and *D*, T1 MR images of the younger sibling in the sagittal (*C*) and coronal (*D*) planes demonstrate less severe abnormalities, with hypoplasia of the inferior vermis and the cerebellar hemispheres and secondary enlargement of the cisterna magna in a posterior fossa of normal size. This case resembles the Dandy-Walker variant.

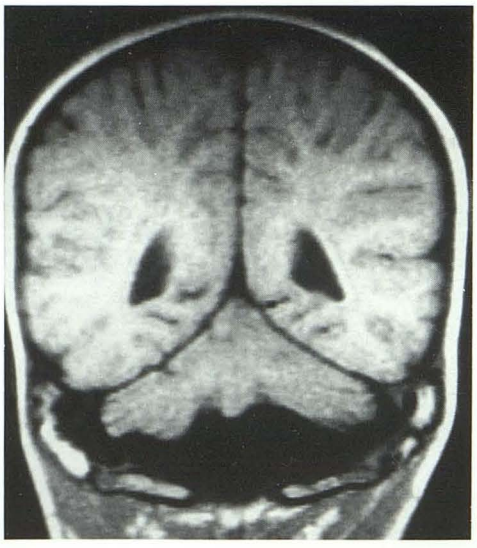

Multiple foci of heterotopic cerebellar cortex are found in the subcortical white matter (2). Associated abnormalities of the cervicomedullary junction include complete absence of the pyramidal decussations, dysplasia of the olivary and para-olivary nuclei, and hypoplasia of the nucleus gracilis, solitary fascicle, and descending trigeminal tracts (46).

Occipital meningoceles or meningoencephaloceles may be present in up to one-third of patients (2). Infrequent cerebral abnormalities include variable degrees of dysgenesis of the corpus callosum and cerebral atrophy (Fig. 25) (46). In some cases, the findings may resemble those of the Dandy-Walker variant or mega cisterna magna.

The embryologic defect in Joubert syndrome has not been determined. The malformation may result from a genetically determined arrest or derangement of the development of the rostral portions of the rhombic lips, with relative sparing of the rest of the alar plates. Thus the vermis would be affected predominantly with more nearly normal cerebellar hemispheres and fourth ventricle (19).

### Tectocerebellar Dysraphia

Tectocerebellar dysraphia refers to the combination of vermian hypoplasia or aplasia, occipital encephalocele, and dorsal traction of the brain stem so that the hypoplastic cerebellar hemispheres come to lie ventral and lateral to the brain stem (Fig. 26) (48). These cases have previously been termed "inverse cerebellum with occipital encephalocele" (49). This disorder has been thought to be a link between the Arnold-Chiari and Dandy-Walker malformations (49, 50), because the dysplasia of the cerebellar vermis, the large fourth ventricle, and the high transverse sinuses seen in this condition are also seen with Dandy-Walker malformation, while the beaked tectum, the kinking of the brain stem, and the position of the cerebellum ventral to the pons seen in this condition are also seen (in milder form) in Chiari II malformation. It should be noted, however, that tectal beaking and kinking of the brain stem are commonly seen in occipital encephaloceles; therefore, the "link" to the Chiari II malformation is, at most, a superficial resemblance.

Tectocerebellar dysraphia is a rare sporadic malformation that more commonly affects males. The patients all present with occipital encephaloceles, and may be microcephalic (49). The children usually die within the first year of life, but may survive to age 8 years. Children who survive the neonatal stage usually require shunting for hydrocephalus. Tectocerebellar dysraphia shows similarities to Walker-Warberg syndrome, an autosomal recessive disorder, with agyria, hydrocephalus, and retinal dysplasia.

Pathologically, these infants demonstrate an occipital encephalocele that contains cerebellar cortex. There is associated deformation of the tectum, such that the posterior colliculi form long, thin, peg-shaped processes that project towards the bony defect (Fig. 26). The vermis is absent or severely hypoplastic, with small remnants of

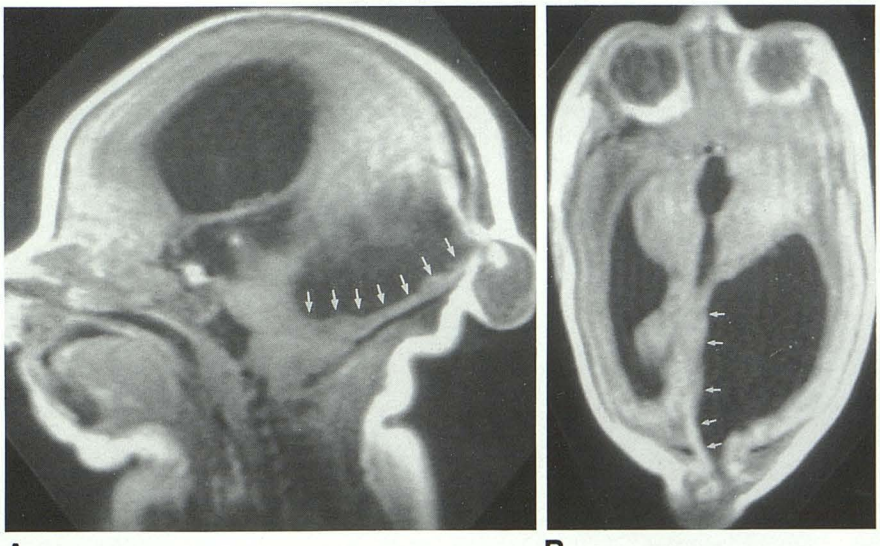


Fig. 26. Tectocerebellar dysraphia. T1 MR in the sagittal (*A*) and axial (*B*) planes demonstrate long peg-shaped processes extending from the tectum of the midbrain to the occipital encephalocele (*arrows*). There is poor differentiation of the brain stem from the cerebellum due to the ventral orientation of the cerebellar hemispheres. Supratentorially, there is marked hydrocephalus and dysplasia of the corpus callosum in the region of the splenium. The smooth interface between gray and white matter indicates agyria.

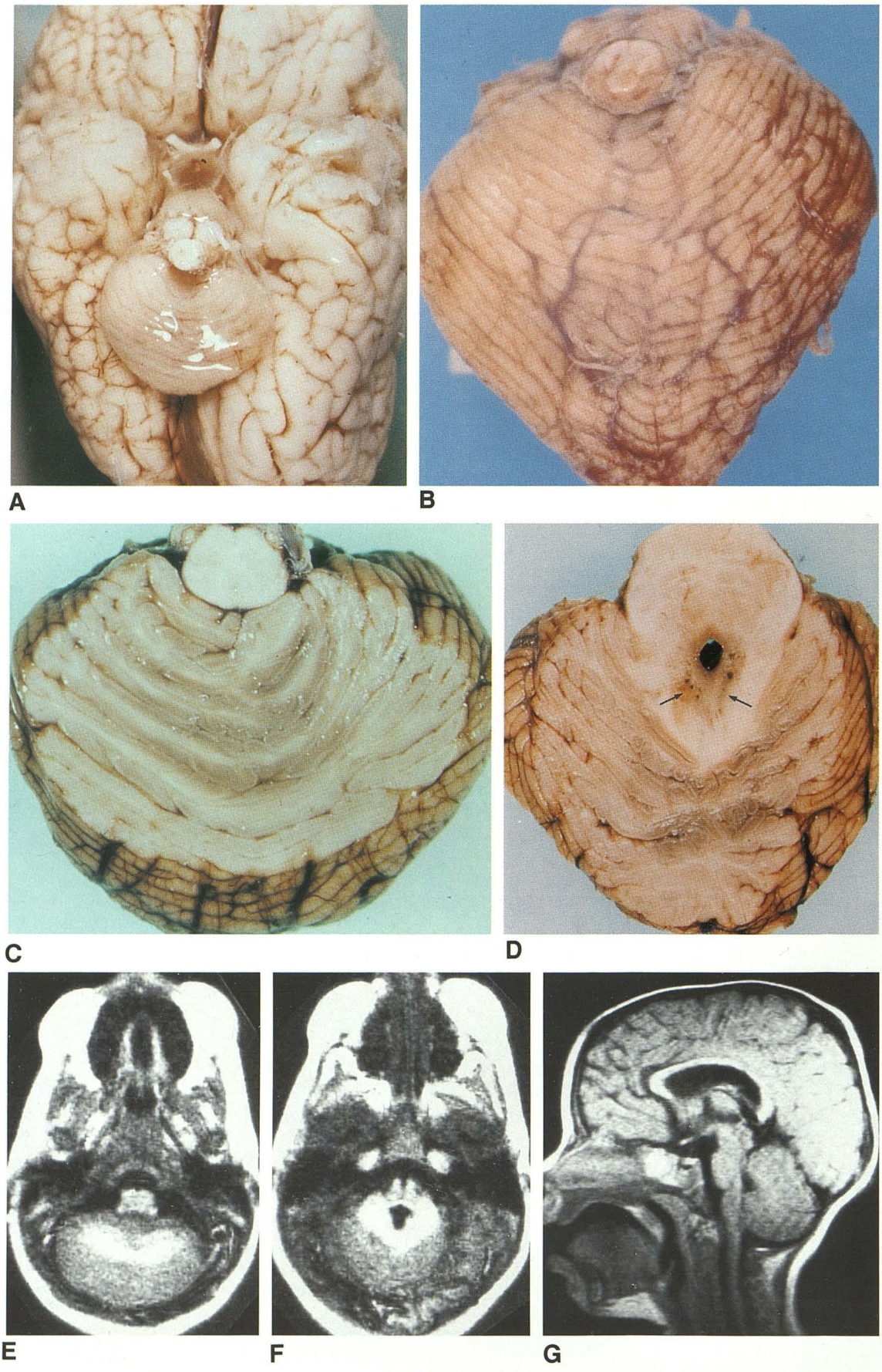
A
B
C
D
E
F
G

the superior vermis. The cerebellar hemispheres are rotated ventrally and may come to lie ventral to the brain stem due to hypoplasia/absence of the vermis. The posterior fossa is small and shallow. Variably associated supratentorial malformations include fusion of the thalami, anomalous cerebrocortical convolutions termed polymicrogyri by Smith (50), dysplasia of the mammillary bodies, and aplasia of the corpus callosum. The atlas and the occipital squama may be bifid. There is occasional cervical hydromyelia (2). Tectocerebellar dysraphia is distinguished from simple traction deformities secondary to dislocation of cerebellar tissue into an occipital cephalocele by the severity of the deformities, their complexity, and the severe hypoplasia/aplasia of the vermis (2).

Embryologically, this disorder is believed to result from an insult early in embryogenesis at the 10- to 30-mm stage. Defects of dorsal induction and neuroschisis cause an encephalocele that pulls the brain stem tightly against the posterior aspect of the calvarium. Consequently, the tectum and the cranial nerves become elongated and the cerebellar hemispheres assume a ventral position (50). Most likely, the encephalocele results in separation of the cerebellar hemispheres, preventing their fusion in the midline and thereby blocking formation of the vermis.

## Rhombencephalosynapsis

The term rhombencephalosynapsis signifies a hypoplastic single-lobed cerebellum, with vermian hypogenesis or agenesis and fusion of the cerebellar hemispheres, cerebellar peduncles, and the dentate nuclei (Fig. 27) (19). This disorder was first described by Obersteiner (1916) (51) on the postmortem examination of a normal 28-year-old suicide victim (52). DeMorsier named the disorder rhombocephalosynapsis (53), which was changed to rhombencephalosynapsis by Gross (54). To date, 17 cases have been reported (19).

Clinically, these children present with signs of cerebellar and motor dysfunction (55). Rhombencephalosynapsis appears to be one of the few posterior fossa malformations that present with "cerebellar signs." The intellectual impairment and life expectancy are variable. Those children with a rudimentary cerebellum appear to do worse. The oldest patient recorded has survived to 35 years of age. The vast majority die in infancy and childhood.

Pathologically, all reported cases demonstrate a single-lobed cerebellum. The single cerebellum is typically hypoplastic but may vary significantly in size. The folia and fissues are oriented transversely. If the hypoplasia of the two hemicerebelli is symmetrical, the folia and fissures extend directly across the midline. If the hemicerebelli are asymmetric, the folia and fissures angle across the midline. The vermis is absent or very hypoplastic. The flocculi are usually present, however rudimentary. The tonsils are usually fused. All cases show characteristic apposition or fusion of the dentate nuclei, forming a horseshoe-shaped arc across the midline. The inferior olivary nuclei are usually absent. The colliculi are usually fused.

The posterior fossa is small; there is no cyst present. The fourth ventricle has variable size. Its typical keyhole shape (Fig. 27) results from the dorsal and rostral convergence of the dentate nuclei, the cerebellar peduncles, and the inferior colliculi (tectal fusion) (2, 19). Associated supratentorial malformations include abnormal gyri,

Fig. 27. Rhombencephalosynapsis.

*A*, Uncut postmortem specimen of the inferior surface of the brain demonstrates the hypoplastic single-lobed cerebellum. Absence of the paravermian sulci, posterior cerebellar notch, and any interruption in the course of the folia and fissures indicates that the vermis is not present as a defined structure.

*B*, Inferior surface of a second specimen oriented like *A* shows union of the folia and fissures of the hemispheres across the midline with no delineation of a vermis.

*C* and *D*, Axial sections at the level of the medulla (*C*) and the upper pons (*D*) show that the folia and fissures cross the midline with no differentiation of vermis (*C*), that the middle cerebellar peduncles converge into a central mass of white matter (*D*) and the dentate nuclei (*arrows*) fuse together in a horseshoe configuration.

*E–G*, 13-month-old child with ataxia and developmental delay.

*E* and *F*, Inversion recovery axial MR images at the level of the midmedulla (*E*) and pons (*F*) demonstrate continuity of the gray and white matter of the folia across the midline of the single lobe of the cerebellum. The cerebellar peduncles converge and fuse. The dentate nuclei are not resolved. Specimens and MR both show a small, narrow fourth ventricle with a "keyhole" shape.

*G*, Midsagittal T1 MR shows the small brain stem, small fourth ventricle, and a cerebellar—not vermian—configuration of the midline with no definition of vermian lobules. The posterior fossa and cisterna magna are small.

fused cerebral peduncles, fused thalami, fused fornices, hypoplasia of the temporal lobes (particularly in the regions of the hippocampal formations), hypoplasia of the optic chiasm, and thinning of the corpus callosum (2). An association with hydrocephalus and with septo-optic dysplasia has been described (19, 56).

Embryologically, rhombencephalosynapsis is likely to represent an early developmental derangement, probably occurring at stages 14–17 (28–41 days gestation) (Fig. 28) (19, 42). Since the dentate and olivary nuclei, the peduncles, and the flocculi do not begin to appear until stages 18–19 (approximately 44 and 48 days) (19), the derangements of these structures that are seen in rhombencephalosynapsis should arise in the preceding stages. Depending on the specific insult, the primordia for these structures could fail to develop or develop hypoplastically (19). Slight differences in the cause or extent of the insult could then lead to the variable abnormalities of the superior, middle, and inferior cerebellar peduncles, the dentate, and the olivary nuclei (19).

As in some of the low occipital encephaloceles and in tectocerebellar dysraphia, the key pathologic feature is the fusion of the tectum. Absence or hypoplasia of the normal midline vermis and absence of distension of the rhombencephalic vesicle permits the primordia for the cerebellar hemispheres to fuse together, across the midline into one structure. This fusion of two lateral primordia for the cerebellar hemispheres into one single-lobe cerebellum in rhombencephalosynapsis is conceptually distinct from the holoprosencephalies, where failure of diverticulation leads to persistence of the initially single prosencephalon rather than formation of two telencephalic hemispheres.

## Other Conditions with Vermian Aplasia

Vermian agenesis has been observed with fetal alcohol syndrome, Goldenhar-Gorlen syndrome, and Warfarin syndrome among others (1).

### *Neocerebellar Dysgenesis*

Dysgeneses involving the neocerebellum include the developmental defects of aplasia, hypoplasia, and dysplasia of the entire cerebellum or of one or both hemispheres. In the aplasias, the neocerebellum is underdeveloped in whole or in part. The aplasias include primary nonformation of the neocerebellum *and* lesions that result from damage to the cerebellar anlage early in embryogenesis (3). In the *hypoplasias*, the entire neocerebellum or part of it is smaller than normal but the individual folia are grossly and micro-

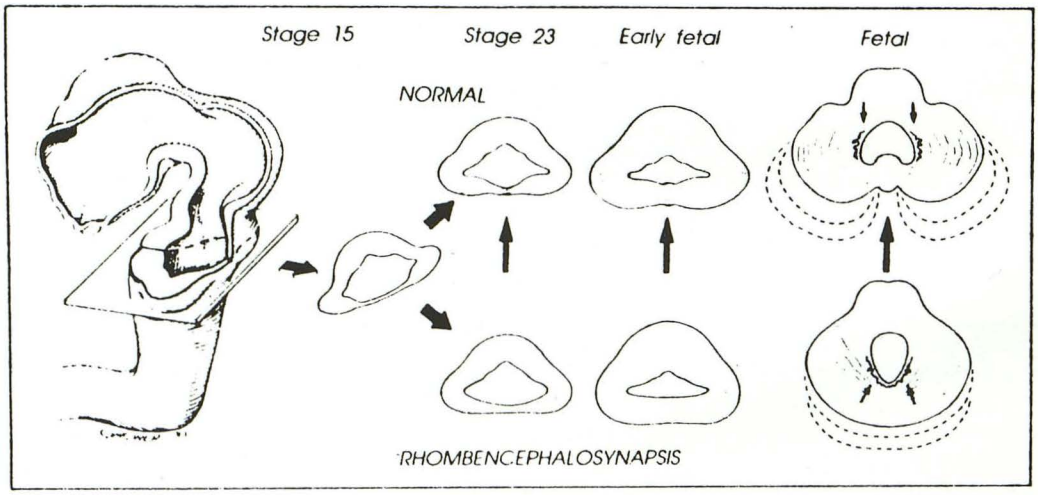


Fig. 28. Proposed embryogenesis of rhombencephalosynapsis. Diagrammatic representation of cerebellar embryogenesis in the normal and in rhombencephalosynapsis. At approximately Carnegie stage 15, the embryo has the shape shown on the left. Axial section through the embryo near to the junction of the isthmic segment and rhombomere 1 shows the rhombic lips converging to the midline dorsally. In the normal brain, embryogenesis proceeds to form the vermis (*long arrows*), cerebellar hemispheres, and fourth-ventricle as shown at late embryonic, early fetal, and fetal stages. The dentate nuclei (*small arrows*) normally develop lateral to the fourth ventricle. In rhombencephalosynapsis, absence of the vermis results in abnormal cerebellar hemispheric fusion, malorientation of folia, and a "fused" horseshoe-shaped dentate nucleus (*small arrows*) that appears to be draped posterior to the fourth ventricle. *Broken lines* dorsally represent the pattern and extent of future cerebellar growth in each case. (Reprinted with permission from Truwit et al (19).

scopically normal in appearance (Fig. 30) (52). Both neocerebellar aplasia and neocerebellar hypoplasia are characterized by a small vermis and extreme smallness or absence of the cerebellar hemispheres except for persistent flocculi (1). Neocerebellar hypoplasia is far more common than aplasia. The neocerebellar dysplasias (synonym: heteroplasias) include abnormalities of the folia such as allogyria, microgyria, macrogyria, polygyria, and agyria. These are frequently microscopic and are seen histologically in the presence of heterotopias (52).

Neocerebellar changes may coexist with paleocerebellar malformations, as in cases of hemispheric defects with agenesis of the inferior vermis (1). Some cases of neocerebellar dysplasia appear to conform more closely to defects of the anterior or of the posterior lobes of the cerebellum than to the topography of the paleocerebellum versus neocerebellum. These disorders still have unsatisfactory nosologic definition (2).

Clinically, cerebellar hypoplasia is usually an isolated, sporadic anomaly. However, it may also be seen in Werdnig-Hoffmann syndrome, an autosomal recessive disorder (57), and in rare families (1), suggesting a genetic basis.

Patients with cerebellar aplasia and hypoplasia may show no or few symptoms (3). With severe cerebellar hypoplasia or aplasia, there is a disabling degree of irregularity of movement characteristic of cerebellar ataxia, especially in the finer movements of the hand. Before modern neuroimaging, the majority of these cases were considered incidental observations at postmortem examination. Attempts have been made to explain the absence of clinical symptoms on the basis of functional compensations in the neural structure (21).

Pathologically, neocerebellar aplasia is associated with large cortical defects that are usually bilateral and roughly symmetrical (Fig. 29) (1). Fibrotic white matter abuts the surface (1). Normal cerebellar cortex is seen at the periphery of the defect (1). The zone of transition may show atrophy of the cortex, shrunken gyri, heterotopic tissue, or disorganization of cortical structure (1). The flocculonodular lobe is present, since this developed with the archicerebellum earlier in embryogenesis.

The dentate nucleus is severely affected and may be absent or disorganized (1). The roof nuclei are better preseverd. In the brain stem, the pontine gray matter is often involved (1). Brain-stem nuclei may be hypoplastic or absent (1). The olives may be hypoplastic.

In neocerebellar hypoplasia/dysplasia, the cortex is not absent, but is poorly developed with fewer than normal folia (Fig. 30). Unilateral cerebellar hypoplasia is more common than bilateral hypoplasia (Fig. 31). Unilateral hypoplasia of the cerebellum is associated with hypoplasia of the ipsilateral dentate nucleus and the *contralateral* inferior olivary nuclei and pontine nuclei (Fig. 32) (1). Bilateral cerebellar hypoplasia is associated

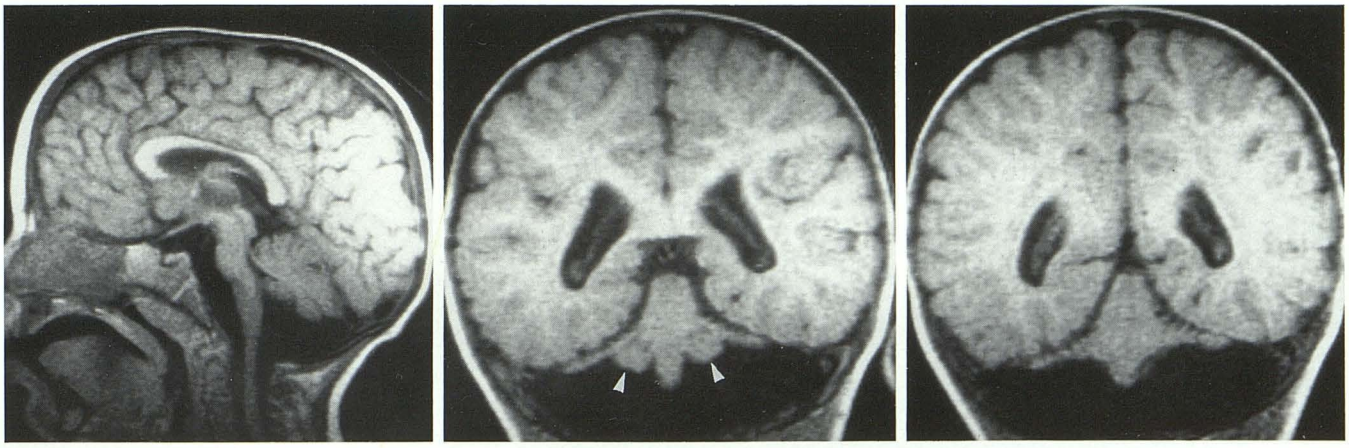


Fig. 29. Severe neocerebellar hypoplasia.

*A*, Midsagittal T1 MR demonstrates a small posterior fossa with secondary enlargement of the cisterna magna. The cerebellar vermis appears to be nearly intact except for mild reduction in the inferior region. The brain stem is hypoplastic.

*B* and *C*, Coronal MR at two levels demonstrates the relatively normal cerebellar vermis and the marked hypoplasia of the cerebellar hemispheres, (ie, neocerebellum). The flocculus of the archicerebellum is identified on each side (*arrowheads*).

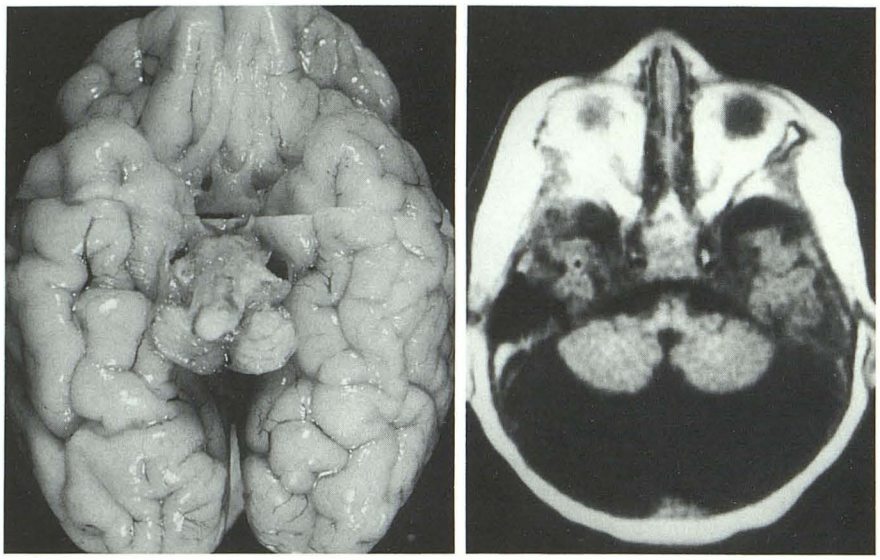


Fig. 30. Cerebellar hypoplasia. *A*, Gross pathologic specimen of the inferior surface of the brain, and *B*, axial T1 MR, demonstrate the marked nearly symmetrical cerebellar hypoplasia with secondary enlargement of the cisterna magna. The brain stem is small.

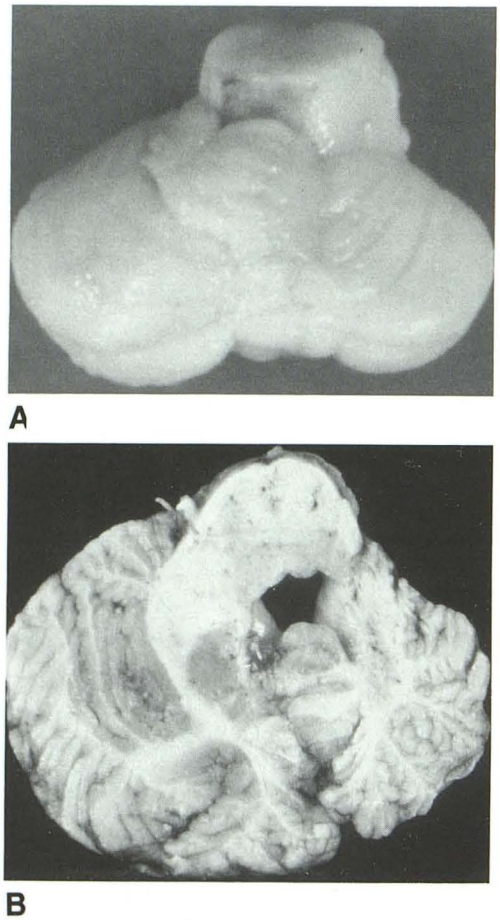


Fig. 31. Unilateral cerebellar hypoplasia; two examples. Gross pathologic specimen of the uncut cerebellum (*A*) and axial section of a second cerebellum (*B*) each show substantial unilateral hypoplasia of one cerebellar hemisphere and the ipsilateral cerebellar peduncles.

with hypoplasia of these nuclei bilaterally and readily appreciable diminution in the brain stem, particularly the pons and medulla.

Embryologically, the lesions may represent an acquired lesion in some cases (1), a genetic defect in others (1). Cerebral malformations such as callosal agenesis and holoprosencephaly may concur (1). The neocerebellar hypoplasias occur somewhat later in the development of the cerebellum, since the neocerebellum forms at the 125-mm stage of the human embryo after the differentiation of the flocculonodular lobe (archicerebellum) (60 days gestation) and predominantly after differentiation of the vermian lobules (approximately 105 days gestation). Concurrent hypoplasia of the brain stem is not explained simply by its similar origin from the rhombic lips. This is illustrated in the asymmetric cases, since neuroblasts do not migrate across the midline. There is probably a sequential failure of development of those nuclei demonstrating neurobiotaxis—the tendency of functionally related areas to establish connection. Lichtenstein (52) feels that the initial defect affects a portion of the nervous system rather than a specific system, ie, a chain of neuronal connections such as seen with olivopontocerebellar degeneration.

Retrograde degeneration of cerebellar neurons can also occur as a consequence of cerebral infarction leading to cortical cerebellar atrophy. This phenomenon, designated *transneuronal* degeneration, appears to cause death of neurons anatomically distinct from, but functionally related to, the neurons that were initially damaged.

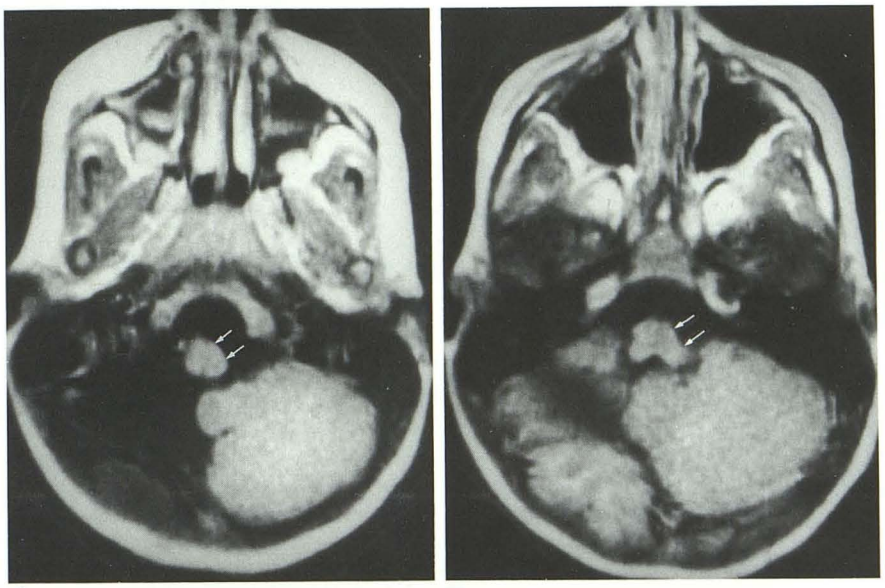


Fig. 32. Unilateral agenesis of the cerebellum. Axial MR at the level of the low medulla (*A*) and high medulla (*B*) show absence of the right cerebellar hemisphere and absence of the contralateral inferior olivary nucleus (*arrows*).

It occurs at a variable time following the death of the primary neurons. Crossed cerebellar atrophy (crossed cerebellar diaschisis) is a case in point, in which contralateral atrophy of the cerebellar hemisphere follows a cerebral infarction (Fig. 33) (58).

Recently, crossed cerebellar diaschisis has also been demonstrated postictially, possibly due to neuronal necrosis of the cerebral hemisphere and *contralateral* cerebellum (59). This idea is supported by cases of experimental hemiconvulsions where measurements of glucose consumption by PET and SPECT imaging show increased neuronal activity in the ipsilateral basal ganglia and thalamus and the contralateral cerebellar cortex (60, 61). Thus neurobiotrophic effect and transneuronal phenomena both refer to degenerative processes. However, the etiology in cerebellar hypoplasia is developmental, not atrophic. Lichtenstein (52) feels these can be differentiated histopathologically. Rarely, aplasia of the pons may occur with relatively normal-looking cerebellar hemispheres (Fig. 34).

Diffuse cerebellar atrophy may be identified in patients following long-term Phenytoin therapy (62). Friedreich ataxia and Ramsay Hunt disease may also demonstrate changes secondary to atrophy of the dentate nucleus, which is the primary disorder in these cases (52). In cases of crossed cerebellar atrophy, the findings clinically are usually related to the cerebral abnormalities.

*Embryogenesis of the Cerebellar Cortex*

The adult cerebellar cortex has three layers: the outer molecular layer, the intermediate Purkinje cell layer, and the inner granule cell layer. In the fetus and during the first 12 months of postnatal life, a fourth *external* granular cell layer is present external to the molecular cell layer. From medial toward lateral, the paired deep fastigial, globus, emboliform, and dentate nuclei lie in relation to the roof and lateral walls of the fourth ventricle. Embryologically, the cells that establish these layers and nuclei migrate to their final sites by two major pathways (Fig. 35):

1. The neurons of the deep cerebellar nuclei and the intermediate Purkinje cell layer of the cerebellar cortex arise in the germinal matrix in the wall of the fourth ventricle from 9–13 weeks and migrate outward—radially—directly to their final sites (18). Distinct portions of the cerebellar primordia give rise to the Purkinje cells populating the hemispheres, the anterior vermis, and the posterior vermis (2).

2. The neurons that will form the molecular and inner granular cell layer arise in a germinal zone in the lateral portion of the rhombic lips. At 11–13 weeks, these cells begin to migrate tangentially over the surface of the cerebellum to form a transient *external* granular cell layer (18). These external granular cells proliferate rapidly from the 13th week of gestation to approximately

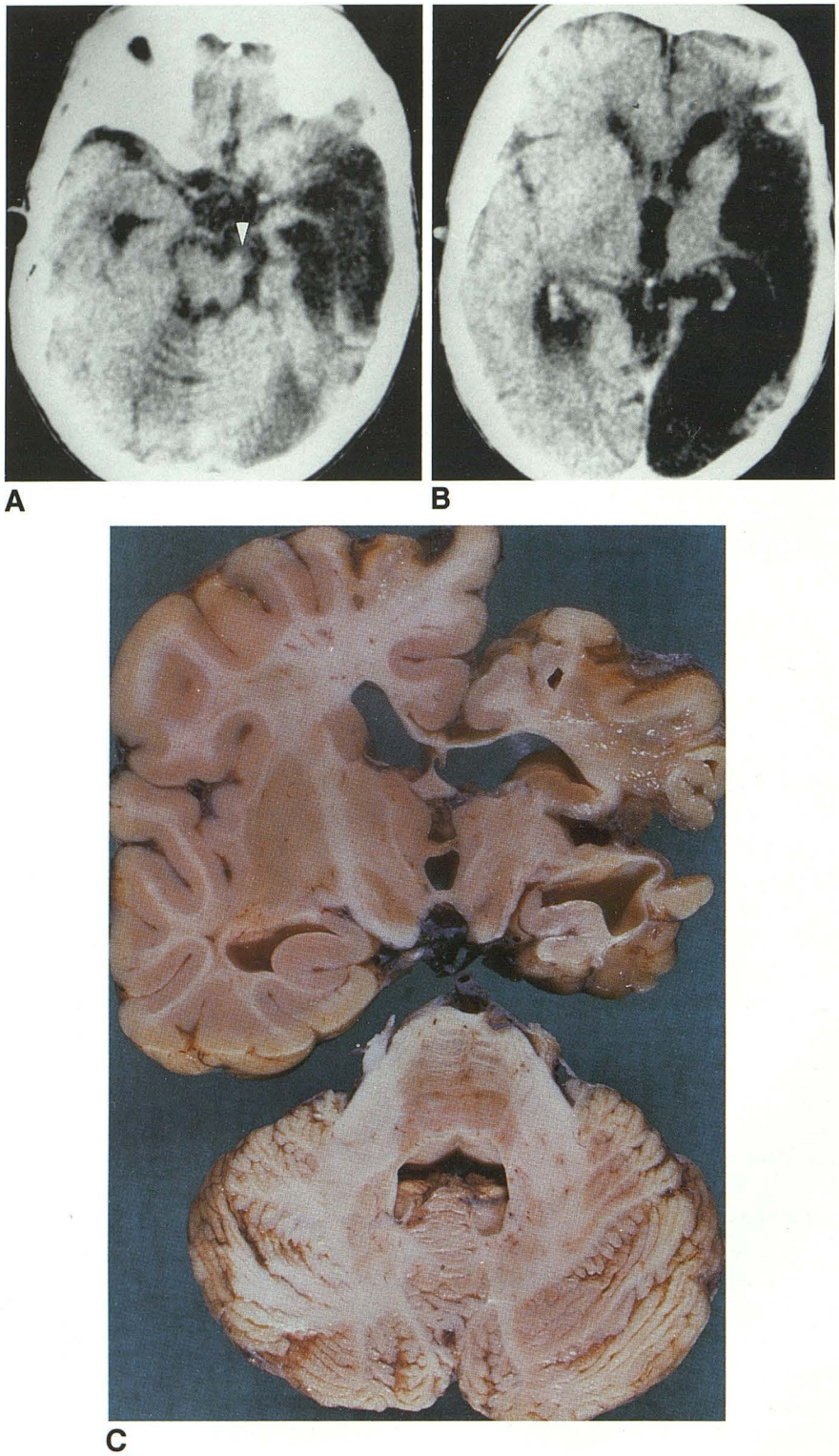


Fig. 33. Crossed cerebellar diaschisis (crossed cerebellar atrophy); 17-year-old boy.

*A* and *B*, axial CT images show extensive postinfarction encephalomalacia in the left cerebral hemisphere, atrophy of the ipsilateral cerebral peduncle (*arrowhead*), and atrophic changes in the contralateral cerebellar hemisphere as indicated by the prominent cerebellar folia.

*C*, Postmortem examination of this patient confirmed the left cerebral atrophy and the contralateral right cerebellar atrophy.

the seventh month postnatally. At approximately the 16th week of gestation, daughter cells begin to migrate inward to form 1) the basket and stellate cells of the molecular cell layer (external to the Purkinje cell layer) and 2) the inner granule cell layer deep to the molecular layer. The external granular cell layer has maximal cell numbers during the first few postnatal months, diminishes

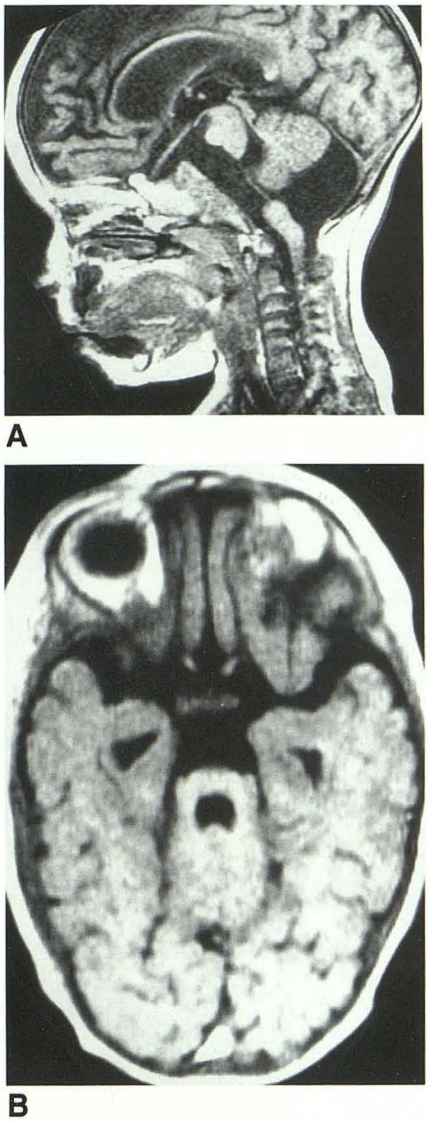


Fig. 34. Agenesis of the pons. T1 MR in the sagittal (*A*) and axial (*B*) planes demonstrates nearly complete absence of the pons. The cerebellar vermis appears intact. The posterior fossa is normal in size. The cisterna magna shows secondary enlargement.

in size as the cells migrate inward, and eventually disappears by the end of the first postnatal year (18).

The cerebellar cortex communicates with other portions of the central nervous system via 1) fibers that synapse with the deep cerebellar nuclei, and 2) fibers that extend to the rest of the CNS via the superior, middle, and inferior cerebellar peduncles. Even if some of the migrations of cells are interrupted, afferent and efferent connective white matter tracts still form. Thus the overall appearance of the cerebellum may be roughly normal despite a developmental insult

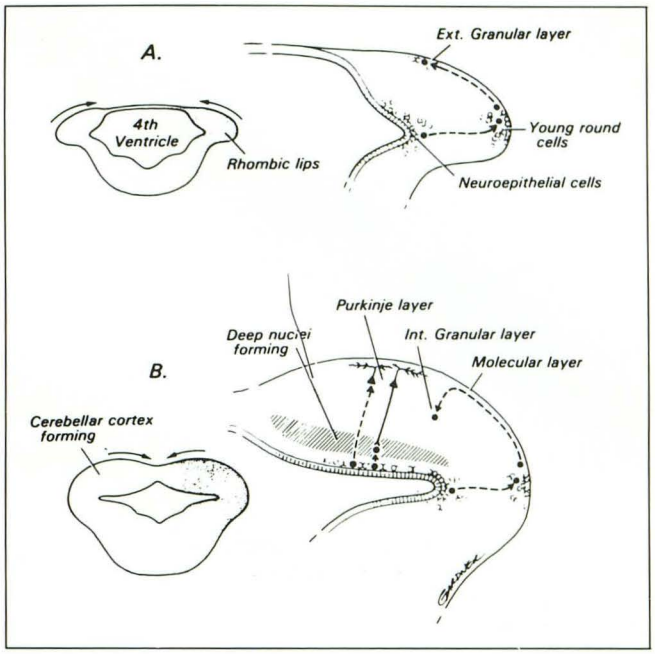


Fig. 35. Diagrammatic representation of the embryogenesis of the layers of the cerebellar cortex. See explanation in text. (Reprinted with permission from Barkovich (34).)

(18). The cerebellum may merely appear hypoplastic (18).

### *Dysplasias of the Cerebellar Cortex*

Lhermitte-Duclos syndrome is a diffuse hypertrophy of the cerebellar cortex that was first reported in 1920 (63). It is classified with the dysplasias of the cerebellar cortex, although it has also been reported confusingly, as Perkinjeoma, gangliocytoma, gangliocytoma amyelinicum diffusum, myelinated neurocytoma, or diffuse dysplastic gangliocytoma dysplasticum (2).

Clinically, Lhermitte-Duclos patients may first present at any age from birth to the sixth decade; most frequently the patients present between the third and fourth decades (64). The male to female ratio is approximately equal (64). A familial case has been reported, although an inheritance pattern has not been identified (63). The presence of associated anomalies, such as megalencephaly, heterotopias, microgyria, hydromyelia, and multiple hemangiomas (65) suggests a dysplastic, possibly genetic origin.

The patients usually have a long-standing history of ill-defined mental or neurologic abnormalities, often related to increased intracranial pressure. Nonsurgical management is associated with poor outcome because the disease is progressive in nature. At present, patients are treated

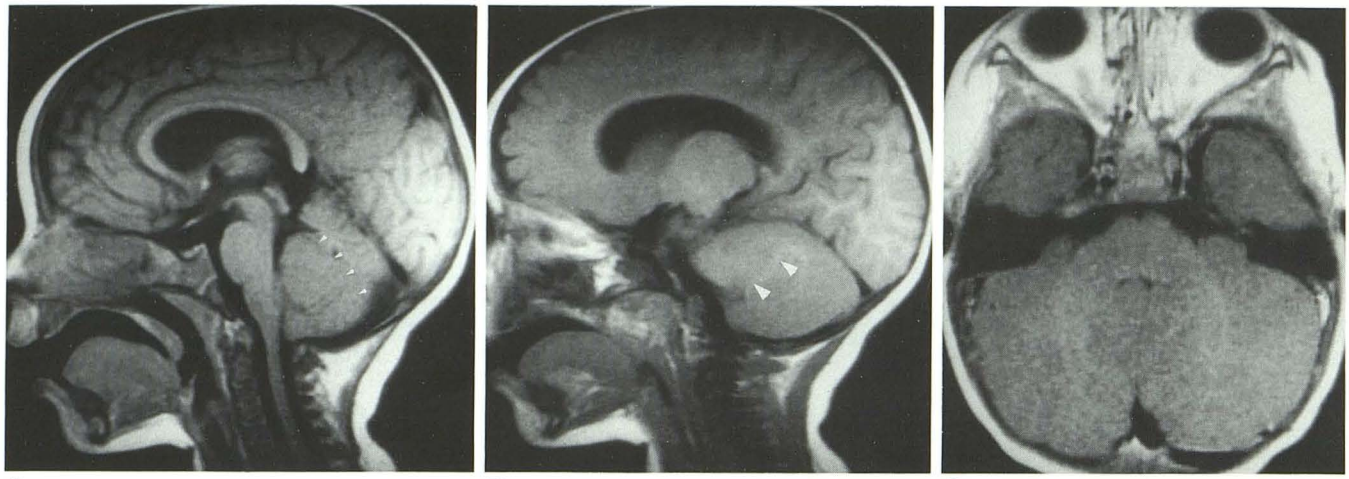


Fig. 36. Diffuse hypertrophy of cerebellar cortex. (Lhermitte-Duclos syndrome).

*A* and *B*, T1 MR in the mid sagittal (*A*) and parasagittal (*B*) planes demonstrates a smooth mass involving the inferior vermis, a clear interface (*arrowheads*) with the normal superior vermis, and upward displacement of the posterior medullary velum and roof of the fourth ventricle. The cerebellar hemisphere is remarkably smooth with thin white matter (*arrowheads*).

*C*, Axial T1 MR shows "filling in" of the posterior fossa and thin attenuated white matter due to the significant thickening or hyperplasia of the cerebellar cortex.

with decompressive surgery for symptomatic relief and to enhance long-term survival. With suboccipital decompression, upper cervical laminectomies, and tissue debulking resection, permanent ventricular shunting is not necessary (66).

Pathologically, the affected portion of the hemisphere exhibits focal, circumscribed enlargement that may extend to the vermis and, occasionally, to the contralateral hemisphere (64, 65). In the affected zone, the folia are broadened and firm. The molecular layer is thickened. Deep to the molecular layer, a thick layer of abnormal large neurons with rounded nuclei and abundant mitochondria replaces the normal inner granular layer. Myelinated fibers arising from the abnormal cells pass into the outer molecular layer, and radiate to the cortical surface, where they form a plexus (2, 64). There is loss of Purkinje cells and absence of Purkinje dendrites (63). The digitations of the white matter within the abnormal folia are thinner than normal, with few or no myelinated fibers. Calcifications are found in the tissue and in the blood vessel walls (2).

Hypertrophy of the involved portion of the cerebellar hemisphere "fills in" the posterior fossa and may cause mass effect, elevated intracranial pressure, and hydrocephalus (Fig. 36) (64). There is no edema and no "invasion" of adjacent areas. Long TR/TE images usually show increased signal intensity in the involved portion of the cerebellar hemisphere (65), but no such signal abnormality could be identified in our case (Fig. 36). No contrast enhancement is seen within the "mass."

Embryologically, Lhermitte-Duclos syndrome appears to result from a disorder of migration of cerebellar neurons (64). Specific disruption of these pathways has not been identified, but the Lhermitte-Duclos syndrome is believed to result from disturbed proliferation and differentiation of granule cell precursors leading to proliferation and hypertrophy of granule cells along the normal path of granule cell migration and at their destination in the depth of the cortex (2).

## Conclusion

In conclusion, the posterior fossa malformations include disorders of paleocerebellar and neocerebellar dysgenesis. These can be conveniently divided into those that have a large posterior fossa and those with a normal posterior fossa. The disorders associated with a large posterior fossa include the Dandy-Walker malformation, mega cisterna magna, and posterior fossa cyst. The disorders associated with small or normal-sized posterior fossa include the Dandy-Walker variant, Joubert syndrome, tectocerebellar dysraphia, rhombencephalosynapsis, the neocerebellar hypoplasias, and cerebellar atrophy. All of these conditions may be associated with increased size of the ventricles and cisterns. When

a normal sized posterior fossa is "filled in," one may consider the diagnosis of dysplasia of the cerebellar cortex, such as is seen with Lhermitte-Duclos syndrome.

Together, the understanding of the embryogenesis, clinical features, and neuroimaging characteristics should lead the neuroimager to a specific diagnosis and should afford the referring clinician, patient, and parents a logical approach to these often perplexing malformations.

## Acknowledgments

We thank Ellsworth C. Alvord, Betty Ann Brody, Keith Fulling, Ronald Lemire, Joseph C. Masdeu, and Lucy B. Rorke for the pathologic correlations.

## References

1. Lemire RJ, Loeser JD, Lecch RW, Ellsworth CA. *Normal and abnormal development of the human nervous system.* Hagerstown, MD: Harper & Row 1975:144–163
2. Friede RL. *Developmental neuropathology.* 2nd ed. Berlin: Springer-Verlag, 1989:347–371
3. Friede RL. *Developmental neuropathology.* New York: Springer-Verlag, 1975
4. England MA. *Color atlas of life before birth: Normal fetal development.* Chicago, Year Book, 1983
5. Arey LB. *Developmental anatomy: A textbook and laboratory manual of embryology.* 5th ed. Philadelphia: Saunders, 1946:429–457
6. Muller F, O'Rahilly R. The first appearance of the future cerebral hemispheres in the human embryo at stage 14. *Anat Embryol* 1988; 177:495–511
7. O'Rahilly R, Muller F, Hutchins GM, Moore GW. Computer ranking of the sequence of appearance of 40 features of the brain and related structures in staged human embryos during the 7th week of development. *Am J Anat* 1988;182:295–317
8. Naidich TP, Pudlowski RM, Naidich JB, Gornish M, Rodriguez FJ. Computed tomographic signs of the Chiari II malformation. I. Skull and dural partitions. *Radiology* 1980;134:65–71
9. Naidich TP, Pudlowski RM, Naidich JB. Computed tomographic signs of the Chiari II malformation. II. Midbrain and cerebellum. *Radiology* 1980;134:391–398
10. Naidich TP, Pudlowski RM, Naidich JB. Computed tomographic signs of the Chiari II malformation. III. Ventricles and cisterns. *Radiology* 1980;134:657–663
11. Naidich TP, McLone DG, Fulling KH. The Chairi malformations. IV. The hindbrain deformity. *Neuroradiology* 1983;25:179–197
12. Curnes JT, Oakes WJ, Boyko OB. MR imaging of hindbrain deformity in Chiari II patients with and without symptoms of brainstem compression. *AJNR* 1989;10:293–302
13. Wolpert SM, Cohen A, Runge VR, Scott RM. Chiari II malformation (letter). *AJNR* 1989;10:1279–1280
14. el Gammal T, Mark EK, Brooks BS. Mr imaging of Chiari II malformation. *AJR* 1988;150:163–170
15. Wolpert SM, Scott RM, Platenberg C, Runge VM. The clinical significance of hindbrain herniation and deformity as shown on MR images of patients with Chiari II malformation. *AJNR* 1988;9:1075–1078
16. Wolpert SM, Anderson M, Scott RM, Kwan ES, Runge VM. Chiari II malformation: MR imaging evaluation. *AJR* 1987;149:1033–1042
17. Yuh WT, Segall HD, Senac MO, Schultz D. MR imaging of Chiari II malformation associated with dysgenesis of cerebellum and brain stem. *J Comput Assist Tomogr* 1987;11:188–191
18. Barkovich AJ, Kjos BO, Norman D, Edwards MS. Revised classification of posterior fossa cysts and cystlike malformations based on the results of multiplanar MR imaging. *AJNR* 1989;10:977–988
19. Truwit CL, Barkovich AJ, Shanahan R, Maroido TV. MR imaging of rhombencephalosynapsis: report of three cases and review of the literature. *AJNR* 1991;12:957–965
20. Brodal A, Hauglie-Hanssen E. Congenital hydrocephalus with defective development of the cerebellar vermis (Dandy-Walker syndrome). *J Neurol Neurosurg Psychiatry* 1959;22:99–108
21. Stewart RM. Cerebellar agenesis. *J Men Sci* 1956;102:67–77
22. Urich H. Malformations of the nervous system, perinatal damage and related conditions in early life. In Blackwood W, Corsellis JAN, eds. *Greenfield's Neuropathology.* Chicago: Yearbook, 1976:377–469
22. Dandy WE, Blackfan KD. Interval hydrocephalus. *Am J Dis Child* 1914;8:406–482
23. Taggart TK, Walker AE. Congenital atresia of the foramina of Luschka and Magendie. *Arch Neurol Psychiatry* 1942;48:583–612
24. Benda CE. The Dandy-Walker syndrome of the so-called atresia of the foramen of Magendie. *J Neuropathol Exp Neurol* 1954;13: 14–29
25. Hirsch JF, Pierre-Kahn A, Renier D. Sainte-Rose C, Hoppe-Hirsch E. The Dandy-Walker malformation. *J Neurosurg* 1984;61:515–522
26. Raybaud C. Cystic malformations of the posterior fossa: abnormalities associated with development of the roof of the fourth ventricle and adjoint meningeal structures. *J Neuroradiol* 1982;9:103–133
27. Murray JC, Johnson JA, Bird TD. Dandy-Walker malformation: etiologic heterogeneicity and empiric recurrence risks. *Clin Genet* 1985;28:272–283
28. Golden J, Rorke LB, Bruce DA. Dandy-Walker syndrome and associated anomalies. *Pediatr Neurosci* 1987;13:38–44
29. Maria BL, Zinreich SJ, Carson BC, Rosenbaum AE, Freeman JM. Dandy-Walker syndrome revisited. *Pediatr Neurosci* 1987;13:45–51
30. Pillay P, Barrett GH, Lanzeiri C, Cruse C. Dandy-Walker cyst upward herniation: the role of magnetic resonance imaging and double shunts. *Pediatr Neurosci* 1989;15:74–79
31. Hart MN, Malamud N, Ellis WG. The Dandy-Walker syndrome: a clinicopathological study based on 28 cases. *Neurology* 1972;22: 771–780
32. Kojima T, Waga S, Shimizu T, Sakakura T. Dandy-Walker cyst associated with occipital meningocele. *Surg Neurol* 1982;17:52–56
33. Asai A, Hoffman HJ, Hendrick EB, Humphreys RP. Dandy-Walker syndrome: experience at the Hospital for Sick Children, Toronto. Pediatr Neurosci 1989;15:66–73
34. Barkovich AJ. Pediatric Neuroimaging. In: Norman D, ed. *Contemporary neuroimaging.* New York: Raven, 1990:115–120
35. Naidich TP, Radkowski MA, Bernstein RA, Tan WS. Congenital malformations of the posterior fossa. In Taveras JM, Ferrucci JT, eds. *Radiology.* Philadelphia: Lippincott, 1986:1–17
36. Carmel DW, Antunes JL, Hilal SK, Gold AP. Dandy-Walker syndrome: clinicopathological features and re-evaluation of modes of treatment. *Surg Neurol* 1977;8:132–138
37. Raimondi AJ, Samiston G, Yarzagarz L, Norton T. Atresia of the foramen of Luschka and Magendie: the Dandy-Walker cyst. *J Neurosurg* 1969;31:202–216
38. Naidich TP, Radkowski MA, McLone DG, Leestma J. Chronic cerebral herniation in shunted Dandy-Walker malformation. *Radiology* 1986; 158:431–434
39. LaTorre E, Fortuna A. Cachipint E. Angiographic differentiation between Dandy-Walker cyst and arachnoid cyst of the posterior fossa in newborn infants and children. *J Neurosurg* 1973;38:298–308
40. Wolpert SM, Haller JS, Rabe EF. The value of angiography in the Dandy-Walker syndrome of posterior fossa extraaxial cysts. *AJR* 1970;109:261–272

41. Harwood-Nash DC, Fitz CR. *Neuroradiology in infants and children.* Vol 3. St. Louis: Mosby, 1976:1014–1019
42. Go KG, Houthoff HJ, Blaauw EH, et al. Arachnoid cysts of the sylvian fissure: evidence of fluid secretion. *J Neurosurg* 1984;60:803–810
43. Gilles FH, Rockeh FX. Infantile hydrocephalus: retrocerebellar "arachnoid" cyst. *J Pediatr* 1971;79:436–443
44. Naidich TP, McLone DG, Radkowski MA. Intracranial arachnoid cysts. *Pediatr Neurosci* 1986;12:112–122
45. Joubert M, Eisenring J, Robb JP, Andermann F. Familian agenesis of the cerebellar vermis. *Neurology* 1969;19:813–825
46. Kendall B, Kingsley D, Lambert SR, Taylor D, Finn P. Joubert syndrome: a clinico-radiological study. *Neuroradiology* 1990;31: 502–506
47. King MD, Dudgeon J. Stephenson JBP. Joubert's syndrome with retinal dysplasia: neonatal tachypnea as the clue to a genetic brain-eye malformation. *Arch Dis Child* 1984;59:709–718
48. Friede RL. Uncommon syndromes of cerebellar vermis aplasia. II. Tectocerebellar dysraphism with occipital encephalocele. *Dev Med Child Neurol* 1978;20:764–772
49. Padget DH, Lindenberg R. Inverse cerebellum morphogenetically related to Dandy-Walker and Arnold Chiari syndromes: bizarre malformed brain with occipital encephalocele. *Johns Hopkins Med J* 1972;131:228–246
50. Smith MT, Huntington HW. Inverse cerebellum and occipital encephalocele: a dorsal fusion defect uniting the Arnold-Chiari and Dandy-Walker spectrum. *Neurology* 1977;27:246–251
51. Obersteiner H. Ein Kleinhirn ohae Wurn. *Arb Neurol Inst (Wien)* 1914; 21:124–136
52. Lichtenstein BW. Maldevelopments of the cerebellum: a pathologic study with remarks on the associated degeneration of the olivary bodies and the pontine and dentate nuclei. *J Neuropathol Exp Neurol* 1943;2:164–177
53. DeMorsier G. Etude sur les dysraphies cranioencephaliques. III. Agenesis du septum lucidum aven malformation du tractus optique: la dysplasie septo-optique. *Schweiz Arch Neurol Psychiatr* 1956;77: 267–292
54. Gross H. Die Rhombencephalosynapsis: eine systemisierte Kleinhirnfehlbildung. *Eur Arch Psychiatry Neurol Sci* 1959;199:537–552
55. Isaac M, Best P. Two cases of agenesis of the vermis of the cerebellum with fusion of the dentate nuclei and cerebellar hemispheres. *Acta Neuropathol (Berl)* 1987;74:278–280
56. Michaud J, Mizrahi EM, Urich H. Agenesis of the vermis with fusion of the cerebellar hemispheres, septo-optic dysplasia and associated anomalies: report of a case. *Acta Neuropathol (Berl)* 1982;56: 161–166
57. Norman RM. Cerebellar hypoplasia in Werdnig-Hoffmann disease. *Arch Dis Child* 1960;36:96–101
58. Strefling AM, Urich H. Crossed cerebellar atrophy: an old problem revisited. *Acta Neuropathol (Berl)* 1982;57:197–202
59. Tan N, Urich H. Postictal cerebral hemiatrophy: with a contribution to the problem of crossed cerebellar atrophy. *Acta Neuropathol (Berl)* 1984;62:332–339
60. Caveness WF. Energy metabolism in focal seizures. In: Mrsulja BB, Rakic LM, Klatzo I, Spatz M, eds. Pathophysiology of cerebral energy metabolism. New York: Plenum, 1979:267–280
61. Kim SM, Park CH, Intenzo CM, Bell R. Redistribution of crossed cerebellar diaschisis. *Clin Nucl Med* 1989;14:290–291
62. Ghatak NR, Santoso RA, McKinney WM. Cerebellar degeneration following long-term phenytoin therapy. *Neurology* 1976;16:818–820
63. Lhermitte J, Duclos P. Sur un ganglioneurone diffus du cortex de cervelet. *Bull Assoc Fr Etude Cancer* 1920;9:99–107
64. Reeder RF, Daunders RL, Roberts DW, Fratkin JD, Cromwell LD. Magnetic resonance imaging in the diagnosis and treatment of Lhermitte-Duclos disease (dysplastic gangliocytoma of the cerebellum). *Neurosurgery* 1988;23:240–245
65. Smith RR, Grossman RI, Goldberg I, Hackney DB, et al. MR imaging of Lhermitte-Duclos disease: a case report. *AJNR* 1989;10:187–189
66. Rorke LB, Forelson MG, Riggs HE. Cerebellar heterotopia in infancy. *Dev Med Child Neurol* 1968;10:644–650
67. Masdeu JC, Dobben GD, Azar-kia B. Dandy-Walker syndrome studied by computed tomography and pneumoencephalography. *Radiology* 1983;147:109–114